Food Chemistry: X 24 (2024) 101898

Contents lists available at ScienceDirect

Food Chemistry: X

journal homepage: www.sciencedirect.com/journal/food-chemistry-x

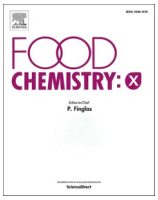

Influence of frozen storage and flavoring substances on the nonvolatile metabolite profile of raw beef: Correlation of lipids and lipid-like molecules with flavor profiles

Sam Al-Dalali [a,b,c,d,*], Zhigui He [a,b,c,*], Miying Du [a,b,c], Hui Sun [a,b,c], Dong Zhao [a,b,c], Cong Li [e], Peijun Li [e], Baocai Xu [e,**]

[a] School of Food and Health, Guilin Tourism University, Guilin, 541006, China
[b] Guangxi Engineering Research Center for Large-Scale Preparation & Nutrients and Hygiene of Guangxi Cuisine, China
[c] Key Laboratory of Industrialized Processing and Safety of Guangxi Cuisine, (Guilin Tourism University), Education Department of Guangxi Zhuang Autonomous Region, China
[d] Department of Food Science and Technology, Faculty of Agriculture and Food Science, Ibb University, Ibb 70270, Yemen
[e] School of Food and Biological Engineering, Hefei University of Technology, Hefei 230601, China

ARTICLE INFO

Keywords:
Frozen storage
Beef
Flavoring substance
Metabolite
LC–MS/MS
Multivariate analysis

ABSTRACT

This study aimed to explore the effects of frozen storage and flavoring substances (sugar and salt) on the metabolite profiles of nonflavored (BS1) and flavored (BS2) beef samples through UHPLC–MS/MS and an untargeted method and flavor profiles using GC–MS and targeted method. Analysis was conducted during 0, 3, and 6 months of frozen storage. A comprehensive analysis of biochemical databases yielded a total of 1791 metabolites: 1183 metabolites were identified in positive ion mode and 608 in negative ion mode. There were 3 categories of metabolites under superclass classification, accounting for 77.93 % of the total metabolites, including lipids and lipid-like compounds (502 species, 33.87 %), organic acids and derivatives (459 species, 30.97 %), and organoheterocyclic compounds (194, 13.09 %). Multivariate statistical analysis showed that after 0, 3, and 6 months of frozen storage, 120, 106, and 62 differential metabolites, respectively, were identified in the comparison between the BS1 and BS2 samples. The results indicated that frozen storage has a decreasing effect on the differential metabolites, while the flavoring substances mainly enhance the metabolite profiles. It can be concluded that flavoring substances and frozen storage primarily influence the metabolites. At 0 and 6 months of frozen storage, 27 volatiles were detected. The correlation analysis displayed a positive correlation between lipids and lipid-like molecules and flavor compounds.

Introduction

Beef is considered an essential bovine product because of its notable attributes, including a high protein content, low fat content, and fatty acid and mineral components (Gu et al., 2021; Jiang et al., 2023). However, a decrease in consumer satisfaction with regular meat has been observed recently, and the demand for meat with enhanced flavor and quality is growing (Felderhoff et al., 2020). The flavor of meat can be enhanced by adding flavoring substances or other additives (Al-Dalali et al., 2022a, 2022b). However, different food flavorings have varied effects on the metabolites of frozen raw beef, and quantitative evidence of the link between flavoring addition and the metabolite of raw beef during frozen storage is lacking. Meat is commonly preserved with salt and sugar. Salt is frequently used in meat production for its preservation, flavor, and antibacterial properties (Overholt et al., 2016). It promotes lipid oxidation in various types of meat, including beef, poultry, and pork (Mariutti & Bragagnolo, 2017). Sugar is often required in the production of processed food aroma compounds because it is a flavor precursor in the Maillard reaction (Al-Dalali et al., 2021).

Metabolomics is an essential field in omics, facilitating the identification of metabolic molecules involved in the growth and maintenance of living organisms (Utpott et al., 2022). Metabolomics is a multifaceted scientific field encompassing the thorough analysis of metabolites and efficiently and rapidly provides results under specific sample conditions.

* Corresponding authors at: School of Food and Health, Guilin Tourism University, Guilin, 541006, China
** Corresponding author.
E-mail addresses: salihsam@gltu.edu.cn (S. Al-Dalali), hzg@gltu.edu.cn (Z. He), baocaixu@163.com (B. Xu).

https://doi.org/10.1016/j.fochx.2024.101898
Received 14 July 2024; Received in revised form 1 October 2024; Accepted 11 October 2024
Available online 12 October 2024

Changes in biological systems can be explored through this technology (Putri et al., 2022; Putri & Fukusaki, 2016). Simultaneously investigating many metabolites enables researchers to identify precise biological alterations and establish connections between metabolites and metabolic processes crucial to phenotypic changes (Putri & Fukusaki, 2016). Metabolomics technologies have attracted substantial interest for their potential use in studies on human illnesses, synthetic biology for the development of valuable products, preharvest raw materials, and postproduction processes (Parijadi et al., 2019; Putri et al., 2022).

Metabolomics has been used in food science as a strong, effective, and sensitive analytical technique (Rizo et al., 2020). Food processing modifies conditions within and outside food components with various processing methods. It changes the metabolic processes of microorganisms and food materials. The fingerprinting, characterization, and transformation of food metabolites and their alteration during food preparation may be successfully determined via metabolomics. According to Lacalle-Bergeron et al. (2021), this use of metabolomics is of great importance to the food sector. The effects of flavoring substances and frozen storage on the quality, safety, and sensory properties of meat can be determined by analyzing the main metabolites (amino acids, proteins, carbohydrates, lipids, and organic acids) and secondary metabolites (toxins, contaminants, and volatile flavor compounds) through metabolomic analysis (Li et al., 2022; Utpott et al., 2022).

Targeted and untargeted metabolomics are the two main analytical methods for metabolomic analysis. According to Utpott et al. (2022) and Lacalle-Bergeron et al. (2021), targeted metabolomics is the study of specific substances in processing or in vivo, whereas untargeted metabolomics compares the metabolite profiles or fingerprints with modifying states. Metabolomics uses nuclear magnetic resonance (NMR) and mass spectrometry (MS). Biology, medicine, and food science utilize NMR and MS-based metabolomics technologies. NMR and MS technologies have rendered metabolomics practical, widespread, and profitable (Pezzatti et al., 2020). MS analysis is used in many fields because it is faster and more sensitive and has a higher resolution and lower maintenance cost than NMR (Li et al., 2022). Changes in metabolites during refrigerated storage at 4 °C, postmortem changes, and dry-aging techniques have been explored. Liu, Hu, et al. (2022) evaluated changes in metabolites from beef exudates (EXUs) to demonstrate their possible use in the evaluation of meat quality; EXUs were obtained from cold meat refrigerated for 2, 4, and 6 days; a total of 433 differential metabolites and 877 metabolites were identified in the EXUs through UPLC–Q–Exactive–MS platform analysis; the differential metabolites were 38 lignans, 19 benzenoids, 22 phenylpropanoids and polyketides, 16 nucleosides, and 17 organic oxygen. Park et al. (2022) studied the change in the metabolite profile of beef after refrigerated storage at 4 °C. Ijaz et al. (2022) studied alterations in the postmortem metabolites of atypical and typically dark, firm, and dry (DFD) beef through UHPLC–Q–TOF/MS; they identified 240 differential chemicals in the comparison among DFD, normal, and typical DFD beef. D-Ribose-5-phosphate, glycerol-3-phosphate, D-glucose-6-phosphate, alpha-D-glucose-1-phosphate, D-fructose-6-phosphate, and dihydroxyacetone phosphate content were higher in atypical DFD beef than in typical DFD and normal beef; additionally, the concentrations of nine amino acids increased in the typical DFD beef. Setyabrata et al. (2022) evaluated and compared the flavor precursors and their release processes in beef subjected to dry-aging techniques, such as standard dry aging, wet aging, UV-light dry aging, and dry aging in a water-permeable bag; the cuts were subjected to a 28-day aging process at a temperature of 2 °C, relative humidity of 65 %, and an airflow rate of 0.8 m/s; all dry-aging samples showed significantly higher levels of reducing sugars and free amino acids ($P < 0.05$); metabolomics analysis showed a significant increase in short-chain peptides in the dry-aged beef ($P < 0.05$). Antonelo et al. (2020) investigated the effects of meat metabolites and metabolic pathways on the tenderness of beef; glucose, lactate, glutamine, and creatine were the key factors for differentiating tender beef from tough beef; this result indicated that metabolic pathways, such as D-glutamate and D-glutamine metabolism, purine metabolism, beta-alanine metabolism, and tricarboxylic acid cycle play an essential role in the assessment of beef tenderness.

In meat marketing, meat is typically stored at low temperatures. However, storage can have beneficial and harmful effects on meat quality. For instance, flavor and softness are enhanced at prolonged aging time, but the stability of color decreases (Ramanathan et al., 2023). Variations in storage conditions might influence the buildup or decrease of some metabolites or substances that affect the attributes of meat quality. Hence, metabolite levels can offer valuable information regarding alterations in quality. To date, no study has elucidated the effects of flavoring substances and frozen storage on the metabolites of raw beef during frozen storage. Thus, the objectives of this study were as follows: (1) to examine untargeted metabolomics and identify raw beef metabolites through MS, (2) to determine the influence of flavoring substances on the profiles of nonvolatile and volatile metabolites in raw beef, (3) to determine the effect of 6 months of frozen storage on nonvolatile and volatile metabolites in raw beef, and (4) to visualize the correlation between lipids and lipid-like compounds and flavors of raw beef through Pearson correlation coefficients and partial least squares regression (PLSR).

Materials and methods

Samples

Three cuts of beef meats were randomly collected from three male Chinese crossbred Xia–Nan cattle (*M. semimembranosus*; 14–15 kg; 7 days postmortem; 24–30 months old) and purchased from the Metro Mall, Hefei City, Anhui, China. The protein content was determined by the Kjeldahl method and the fat content by the Soxhlet method, and their contents were 19.89 ± 1.52 % and 3.37 ± 0.85 %, respectively. Meats were properly wrapped, and stored in an icebox with a temperature of 4 °C until subsequent processing.

Processing of raw beef

Fat and connective tissues were removed from the beef. Subsequently, the meats were cut into fifty-four 8 cm × 4 cm × 2 cm steaks (70.00 ± 2.00 g). The samples were subjected to two different marinade solution treatments with three replicates for each marinade. The steaks were subsequently marinated in one of the two solutions: (1) 25 % cold water (BS1, $n = 9$ steaks × 3 replicates = 27; nonflavored control group) and (2) water with 0.5 % sugar and 2 % salt (BS2, n = 9 × 3 = 27; flavored group).

Three separate batches of raw beef steaks were mixed in a tumbling bowl with the corresponding marinade solution for each treatment. A VT50 vacuum tumbler (Herisau, Switzerland) was used for 2 h at 4 °C. It was programmed for the operating cycle to run for 20 min and then turned off for 10 min. Each treatment had three tumbling replicates and three technical replicates. Using an atmospheric pressure–operated DZ-400/2S-vacuum packer (Shandong, China), we packed each treated beef steak in a polyethylene bag. All operations were performed in a refrigerated room (4 °C).

Freezing and sampling procedure

The packaged steaks were stored at −18 °C in a freezer. Samples were taken at different frozen storage times (3 replicates × 2 marinade treatments × 3 tumbling replicates) of 0, 3, and 6 months for further investigation.

Metabolite extraction

The extraction of metabolites from raw beef meat was conducted according to the method described by Li et al. (2022). Briefly, raw beef

(0.5 g) was weighed, sliced into small pieces, frozen in liquid nitrogen, and freeze-dried. The metabolites from a 50 mg sample were extracted using a 400 μL methanol–water solution (4:1, *v*/v) and 0.02 mg/mL *L*-2-chlorophenylalanin as the internal standard. After the solution settled at −10 °C, it was treated with an ultrasound machine (Ningbo Scientz Biotechnology Co. Ltd., Ningbo, China) operated at 40 kHz and 5 °C for 30 min. The samples were left to stand for 30 min at −20 °C. The supernatant was cautiously transferred to sample vials for LC–MS/MS analysis after centrifugation at 13,000*g* and 4 °C for 15 min. The metabolite measurements were processed separately in four replicates for each treatment and at each frozen storage.

UHPLC–MS/MS analysis

The metabolites were separated and analyzed using a UHPLC-Q Exactive HF-X instrument, according to the method described by Li et al. (2022). For the chromatographic analysis of the metabolites, a UHPLC machine was utilized, with an ACQUITY HSS T3 column installed (100 mm × 2.1 mm × 1.8 μm; Waters, Milford, USA). Both mobile phases contained 0.1 % formic acid; mobile phase A contained 95 % water and 5 % acetonitrile; mobile phase B comprised 47.5 % isopropanol, 47.5 % acetonitrile, and 5 % water. A 3 μL injection volume was used, and the 40 °C column temperature was adjusted. The flow rate was 0.4 mL/min, and the gradient of the mobile phase in positive ion was set as follows: 20 % B, 0–3 min; 35 % B, 3–4.5 min; 100 % B, 4.5–6.3 min; 0 % B, 6.4–8 min. The setup for the negative ion was as follows: 5 % B, 0–1.5 min; 10 % B, 1.5–2 min; 30 % B, 2–4.5 min; 100 % B, 4.5–6.3; 0 % B, 6.4–8 min. An ESI source and a Q Exactive HF-X device were used. The capillary temperatures were set at 425 °C and 325 °C. The flow rates of the aux and sheath gases were set at 13 and 50 arb units, respectively. A rolling range of 20–60 V was used as the normalized collision energy for MS/MS. Two settings, 3500 (+) and 3500 (−) V were used for the spray voltage. The resolution of the MS was 60,000, whereas the resolution of the MS/MS was 7500. MS measurements were performed from 70 *m/z* to 1050 m/z. Mass spectral signals were acquired in negative and positive ion scanning modes. The data-dependent acquisition mode was used for data collection. The quality control (QC) sample was randomly introduced to every 5–15 analysis samples, and the reliability and stability of the detection results were evaluated. Extracts from each sample were combined in a ratio of 1:1 for the preparation of QC samples. QC samples were analyzed using the same method as that used for the normal samples.

Volatile flavor analysis by HS–SPME–GC–MS

The beef samples were subjected to HS–SPME at 0 and 6 months of frozen storage according to previously described procedures (Al-Dalali et al., 2021; Sun et al., 2020). A sample weighing 5 g was placed in a 40 mL headspace container, and 10 μL of 0.42 mg/mL 2-methyl-3-heptanone was added as the internal standard (IS). The silicon septum was tightly placed over the bottle. After a 20 min equilibration period at 60 °C in a water bath, the volatile components were absorbed using divinylbenzene–carboxen–polydimethylsiloxane (Supelco, PA, USA) for 40 min at the same temperature. At 250 °C in the Shimadzu GC–MS injection port, volatiles were thermally desorbed in the splitless mode for 5 min. Columns from Agilent Technology, USA, DB–5MS (60 m × 0.25 mm × 0.25 μm) and DB–Wax (30 m × 0.25 mm × 0.25 μm) were used for the individual separation of volatiles. At 2 mL/min flow rate, helium was used as the carrier gas. The oven temperature was set at 40 °C for 3 min and then increased to 200 °C at a rate of 5 °C /min. Then, it was raised to 230 °C in the DB–Wax and 250 °C in the DB–5MS at a rate of 10 °C/min and held at these temperatures for 3 min. The conditions of the MS detector were as follows: the ion source temperature was 230 °C, and the line transfer was 250 °C. At an electron ionization voltage of 70 eV, the mass scan range was set at 50–400 *m/z*. The retention indices (RIs) and mass spectra documented in the NIST 14 database were compared with those obtained from the DB–5MS and DB–Wax columns for the identification of volatiles. For further identification, available authentic compounds were injected into the GC–MS instrument under the same conditions for the samples to verify identification. The semi-quantification of volatiles was performed with the internal standard method, and the concentration was calculated using the following equation:

$$Semi-quantitation = \frac{Peak\ area\ ratio\left(\frac{volatile}{IS}\right) \times \text{con.of IS}}{Sample\ weight} \times 1000$$

The volatile flavor measurements were processed separately in three replicates for each treatment and at each frozen storage.

Data annotation and processing

The data were presented as means ± S.E. The fixed variables were frozen storage periods and flavoring substances, whereas measurement of volatile flavors and differential metabolites were considered random effects. The flavor measurements were conducted at 0 and 6 months of frozen storage. The effect of frozen storage and flavoring substances on the volatile flavor profiles was statistically analyzed by applying a Factorial Completely Randomized Design with 2 factors (marinade solutions and frozen storage). The significant interaction between the two factors was analyzed by Duncan's multiple range test ($P \leq 0.05$) through the SAS software (v9.0). The metabolite measurements were conducted at 0, 3, and 6 months of frozen storage. The effect of flavoring substances on the differential metabolites was statistically analyzed using a *t*-test at each time of frozen storage through SPSS 25.0 (SPSS Inc., Chicago, USA).

The raw data peak was identified and calibrated using Progenesis QI 2.3 (Nonlinear Dynamics, Waters, USA) by following the method described by Li et al. (2022), with some modifications. Briefly, the data matrix was preprocessed. At least 80 % of the metabolic characteristics identified in each given group were retained. After filtering, the minimum value within the data matrix was used to replace any missing value. Additionally, each metabolic fingerprint was normalized to the sum. To minimize inaccurate results resulting from sample preparation and instrument instability, we standardized the response intensities of the MS peaks in the sample with the sum normalization approach to create a normalized data matrix. QC samples with an RSD of more than 30 % were eliminated and then transformed using a logarithmic function (log10). The metabolites were identified using biochemical databases, such as the Human Metabolome Database (HMDB; https://www.hmdb.ca). The Majorbio Cloud Platform (https://cloud.majorbio.com) was used to perform principal component analysis (PCA) and partial least squares discriminant analysis (PLS–DA) with the ropls R package (Version 1.6.2, https://bioconductor.org/packages/release/bioc/html/ropls.html). Fold difference and *t*-test analyses were conducted. The significance of the metabolites was assessed using the variable importance in projection (VIP) derived from the PLS–DA model and the *P* value of the *t*-test, and substances with a VIP of >1 were considered statistically significant. The VIP analyses were conducted using ropls (Version 1.6.2). The differential metabolites in the comparison between samples were subjected to enrichment analysis and functional annotation using the KEGG database.

As the lipids and lipid-like molecules represented the abundant metabolite group, in addition, most of the identified flavors were formed through lipid degradation and oxidation, the correlation between lipids and lipid-like molecules and volatile flavors was examined using the method described by Al-Dalali et al. (2022b), with some modifications, as follows: (1) Lipids and lipid-like molecules were analyzed using PLS-DA to obtain their VIP values, and only those with VIP values greater than 1 were considered; (2) Pearson's correlation coefficients were then calculated between the lipids and lipid-like molecules with VIP >1 and

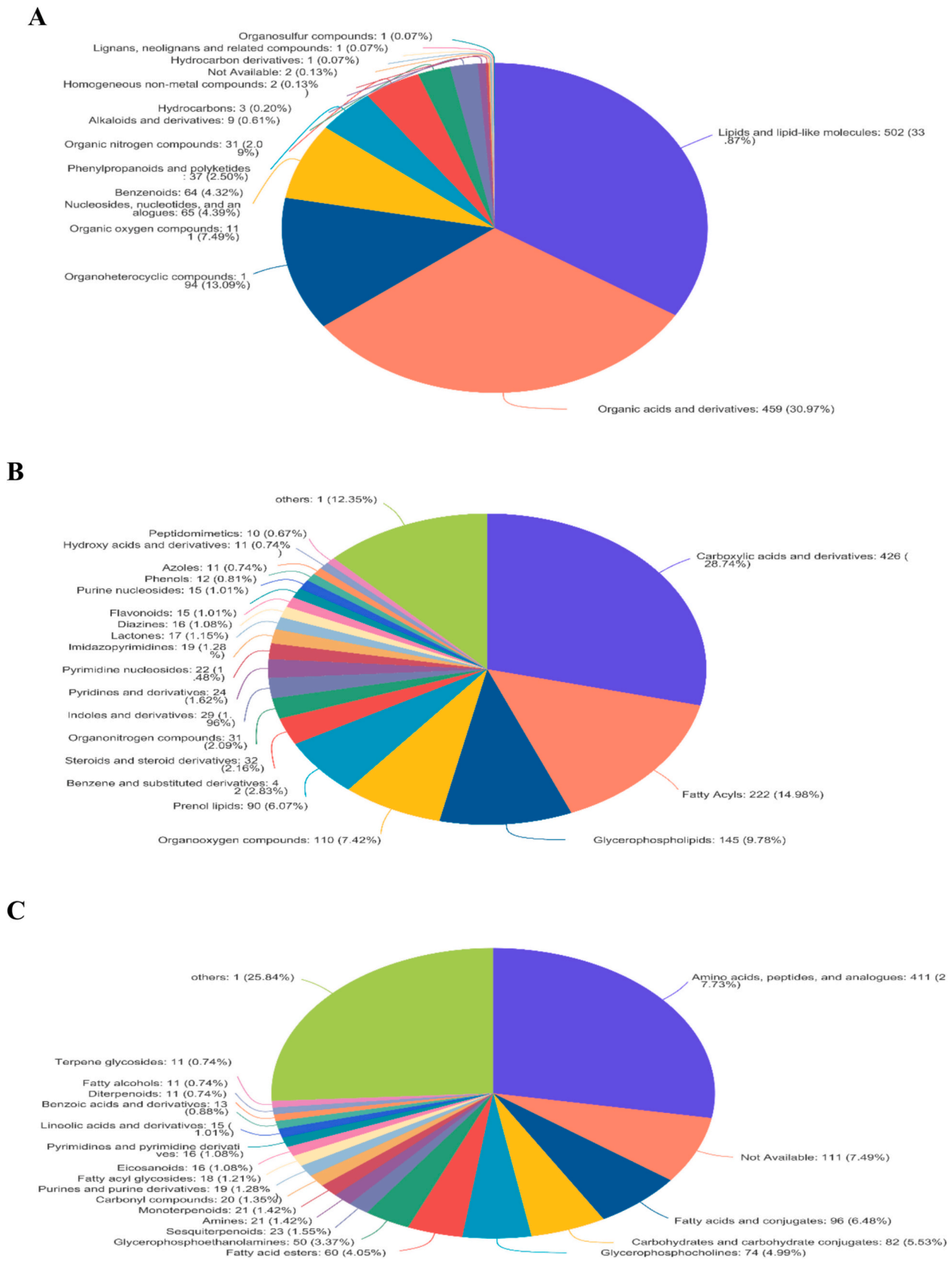

Fig. 1. Metabolite classification: A, superclass level; B, class level; and C, subclass level.

Table 1
120 Differential metabolites between BS1 and BS2 at 0 months of frozen storage.

No.	Metabolite	Formula	VIP_PLS-DA	FC (BS1/BS2)	P_value	BS1	BS2*
1	Pyrroline hydroxycarboxylic acid	C5H7NO3	1.215226926	1.066192803	0.01945	7.20 ± 0.04^{a}	6.75 ± 0.07^{b}
2	Epsilon-(Carboxymethyl)lysine	C8H16N2O4	1.565093097	0.882777692	0.04541	5.74 ± 0.23^{b}	6.50 ± 0.03^{a}
3	Asp Val Lys	C15H28N4O6	1.092688873	0.931606411	0.03564	4.99 ± 0.10^{b}	5.36 ± 0.01^{a}
4	Val Ile	C11H22N2O3	1.175302407	0.940106353	0.04052	6.71 ± 0.12^{b}	7.14 ± 0.02^{a}
5	Spermine	C10H26N4	1.711040605	0.872851733	0.002279	5.99 ± 0.01^{b}	6.86 ± 0.05^{a}
6	Val Lys	C11H23N3O3	1.020208285	1.055928017	0.02485	5.98 ± 0.01^{a}	5.66 ± 0.07^{b}
7	Geniposidic acid	C16H22O10	2.239231182	1.346796657	0.001439	5.80 ± 0.07^{a}	4.30 ± 0.01^{b}
8	Cis-Acetylacrylate	C5H6O3	2.225974758	0.71304683	0.00999	3.69 ± 0.19^{b}	5.18 ± 0.08^{a}
9	Furfural	C5H4O2	1.759954765	0.841335398	0.000788	4.88 ± 0.03^{b}	5.81 ± 0.02^{a}
10	Kaempferol 3-neohesperidoside-7-(2″-p-coumaryllaminaribioside)	C48H56O27	1.601759486	0.887812041	0.001114	6.04 ± 0.02^{b}	6.81 ± 0.03^{a}
11	2-*O*-Alpha-D-Mannopyranosyl-D-Mannopyranose	C12H22O11	1.35376713	0.89298965	0.005416	4.57 ± 0.02^{b}	5.12 ± 0.05^{a}
12	Melezitose	C18H32O16	1.528455783	0.870896754	0.0142	4.74 ± 0.01^{b}	5.45 ± 0.12^{a}
13	Ile Asn	C10H19N3O4	1.353406625	0.906761448	0.03346	5.48 ± 0.08^{b}	6.04 ± 0.12^{a}
14	Ile Ser	C9H18N2O4	1.100328162	0.9340581	0.02915	5.24 ± 0.02^{b}	5.61 ± 0.08^{a}
15	Phosphoribosyl formamidocarboxamide	C10H15N4O9P	1.578462742	0.872591362	0.03357	5.25 ± 0.18^{b}	6.01 ± 0.09^{a}
16	*Cis*-Caffeoyl tartaric acid	C13H12O9	1.025930524	0.942883046	0.005326	5.20 ± 0.01^{b}	5.51 ± 0.03^{a}
17	Ile Gln	C11H21N3O4	1.126622178	0.930275229	0.005759	5.07 ± 0.03^{b}	5.45 ± 0.01^{a}
18	Thr Met	C9H18N2O4S	1.496997446	0.864495376	0.01177	4.29 ± 0.03^{b}	4.97 ± 0.10^{a}
19	Gln Tyr	C14H19N3O5	1.390251395	0.885784873	0.04338	4.66 ± 0.18^{b}	5.26 ± 0.01^{a}
20	Thr Tyr	C13H18N2O5	1.13559052	0.925904652	0.009076	4.83 ± 0.03^{b}	5.22 ± 0.04^{a}
21	17-Hydroxymethylethisterone	C22H30O3	1.208862555	0.909988156	0.04805	4.60 ± 0.11^{b}	5.06 ± 0.09^{a}
22	Ser Leu	C9H18N2O4	1.163019946	0.93349359	0.0301	5.82 ± 0.09^{b}	6.23 ± 0.04^{a}
23	Met Val	C10H20N2O3S	2.339347697	0.694034038	0.00451	3.71 ± 0.10^{b}	5.34 ± 0.11^{a}
24	3'-Amino-3′-deoxythimidine	C10H15N3O4	1.780345537	1.210996871	0.001072	5.41 ± 0.02^{a}	4.47 ± 0.04^{b}
25	Gln Asn Ile	C15H27N5O6	2.317846985	0.682675134	0.000352	3.44 ± 0.02^{b}	5.03 ± 0.03^{a}
26	Trp Glu	C16H19N3O5	1.248313486	0.908308895	0.01464	4.64 ± 0.08^{b}	5.11 ± 0.01^{a}
27	Glu Phe Gly	C16H21N3O6	2.459250645	0.654802909	0.002374	3.42 ± 0.02^{b}	5.22 ± 0.12^{a}
28	Pro Phe Gly	C16H21N3O4	1.375773754	0.879520651	0.000607	4.11 ± 0.02^{b}	4.67 ± 0.01^{a}
29	*P*-Hydroxyphenylethylbiguanide	C10H15N5O	2.011828756	0.789944904	0.01235	4.58 ± 0.18^{b}	5.80 ± 0.05^{a}
30	Leucyl-Tyrosine	C15H22N2O4	1.807199707	0.814883721	0.02314	4.38 ± 0.22^{b}	5.37 ± 0.01^{a}
31	4-(2-Aminopropoxy)-3,5-dimethylphenol	C11H17NO2	2.36269421	0.692406456	0.01254	3.77 ± 0.23^{b}	5.45 ± 0.12^{a}
32	Notoginsenoside R9	C36H62O10	2.367308779	0.683030752	0.02552	3.68 ± 0.02^{b}	5.39 ± 0.39^{a}
33	2-*O*-(6-Phospho-alpha-mannosyl)-D-glycerate	C9H17O12P	2.5245862	0.74095651	0.007956	5.46 ± 0.24^{b}	7.38 ± 0.01^{a}
34	PG(i-14:0/i-13:0)	C33H65O10P	2.68446661	0.604865463	5.83E-05	3.28 ± 0.02^{b}	5.42 ± 0.01^{a}
35	Methionyl-Threonine	C9H18N2O4S	1.583047513	0.801833928	0.04417	3.14 ± 0.02^{b}	3.92 ± 0.23^{a}
36	Phenylalanylglycine	C11H14N2O3	1.551457374	0.805232558	0.02907	3.04 ± 0.11^{b}	3.78 ± 0.15^{a}
37	Ser Val Leu	C14H27N3O5	1.827082604	0.767275248	0.01381	3.31 ± 0.02^{b}	4.32 ± 0.17^{a}
38	Tomatine	C50H83NO21	2.491418119	0.663777537	0.008071	3.67 ± 0.18^{b}	5.53 ± 0.14^{a}
39	Phe Leu	C15H22N2O3	3.172872696	0.301821536	0.01223	1.30 ± 0.45^{b}	4.33 ± 0.13^{a}
40	3'-Amino-3′-deoxythimidine glucuronide	C16H23N3O10	1.831102642	0.776745191	0.03421	3.59 ± 0.06^{b}	4.62 ± 0.27^{a}
41	Leu Pro Ile	C17H31N3O4	1.425757671	0.877347418	0.03457	4.48 ± 0.16^{b}	5.11 ± 0.03^{a}
42	Valylproline	C10H18N2O3	1.166211474	0.878443114	0.002946	2.93 ± 0.02^{b}	3.33 ± 0.02^{a}
43	Kuwanon F	C25H26O6	1.558144164	0.863804589	0.0191	4.66 ± 0.11^{b}	5.40 ± 0.09^{a}
44	Gln Ile	C11H21N3O4	1.243062436	0.923413922	0.02643	5.69 ± 0.10^{b}	6.16 ± 0.02^{a}
45	Prostaglandin PGE2 glyceryl ester	C23H38O7	1.733969513	0.810238487	0.0308	3.94 ± 0.22^{b}	4.86 ± 0.06^{a}
46	3-Pyridinamine	C5H6N2	1.263823266	1.085549964	0.001429	6.04 ± 0.01^{a}	5.56 ± 0.02^{b}
47	*D*-Pipecolic acid	C6H11NO2	1.136472075	1.063667935	0.002099	6.43 ± 0.01^{a}	6.04 ± 0.01^{b}
48	Phe Lys	C15H23N3O3	1.875605338	0.797204136	0.0109	4.16 ± 0.02^{b}	5.22 ± 0.15^{a}
49	PE(20:3(8Z,11Z,14Z)/18:4(6Z,9Z,12Z,15Z))	C43H72NO8P	1.823275106	0.808632827	0.04818	4.36 ± 0.33^{b}	5.39 ± 0.02^{a}
50	Trandolapril-d5 Diketopiperazine	C24H32N2O4	1.985546671	1.306220096	0.03517	5.18 ± 0.32^{a}	3.97 ± 0.04^{b}
51	PS(14:1(9Z)/22:0)	C42H80NO10P	2.106545078	0.767869535	0.01556	4.42 ± 0.23^{b}	5.76 ± 0.01^{a}
52	13'-Carboxy-gamma-tocopherol	C28H46O4	1.065453471	1.068810916	0.04514	5.48 ± 0.09^{a}	5.13 ± 0.05^{b}
53	3-(2-Heptenyloxy)-2-hydroxypropyl undecanoate	C21H40O4	1.326987459	0.870225269	0.01363	3.55 ± 0.08^{b}	4.08 ± 0.02^{a}
54	Val Val	C10H20N2O3	1.213492816	0.932311428	0.01823	6.14 ± 0.07^{b}	6.58 ± 0.04^{a}
55	Oleyl alcohol	C18H36O	1.057184836	0.931308318	0.04057	4.69 ± 0.07^{b}	5.03 ± 0.07^{a}
56	5-Fluorouridine	C9H11FN2O6	1.613185043	1.135821669	0.01549	6.57 ± 0.01^{a}	5.78 ± 0.14^{b}
57	9,12-Octadecadiynoic Acid	C18H28O2	1.383820225	0.883624108	0.03077	4.45 ± 0.14^{b}	5.04 ± 0.03^{a}
58	*P*-Coumaroyl 3-hydroxytyrosine	C18H17NO6	1.15586165	0.919207921	0.02709	4.64 ± 0.07^{b}	5.05 ± 0.06^{a}
59	Biocytin	C16H28N4O4S	2.311954768	0.712583499	0.001893	3.94 ± 0.02^{b}	5.53 ± 0.09^{a}
60	Blumealactone B	C20H28O6	1.81143685	0.802476415	0.02891	4.08 ± 0.08^{b}	5.08 ± 0.23^{a}
61	Met Trp	C16H21N3O3S	1.714931965	0.799086758	0.005529	3.49 ± 0.02^{b}	4.37 ± 0.09^{a}
62	25-*O*-Desacetyl rifabutin	C41H56N4O11	1.370282527	0.867871392	0.006818	3.69 ± 0.02^{b}	4.26 ± 0.06^{a}
63	Met Phe	C14H20N2O3S	1.576474068	0.839463436	0.003865	3.88 ± 0.05^{b}	4.62 ± 0.04^{a}
64	PE(20:5(5Z,8Z,11Z,14Z,17Z)/18:4(6Z,9Z,12Z,15Z))	C43H68NO8P	2.116470644	0.729648843	0.01594	3.65 ± 0.02^{b}	5.01 ± 0.24^{a}
65	Tyr Phe	C18H20N2O4	1.334152483	0.873408933	0.03109	3.77 ± 0.02^{b}	4.32 ± 0.14^{a}
66	(3*S*)-3,6-Diaminohexanoate	C6H14N2O2	1.516280373	0.84800353	0.006733	3.84 ± 0.05^{b}	4.53 ± 0.06^{a}
67	Ile Leu	C12H24N2O3	1.469184046	0.90003034	0.02577	5.93 ± 0.11^{b}	6.59 ± 0.10^{a}
68	Thr Trp	C15H19N3O4	1.140745043	0.917841815	0.03663	4.49 ± 0.10^{b}	4.89 ± 0.05^{a}
69	Cucurbitacin C	C32H48O8	1.912925501	0.807581655	0.04393	4.77 ± 0.34^{b}	5.90 ± 0.05^{a}
70	Asn Trp	C15H18N4O4	1.721959743	0.84587188	0.001454	4.84 ± 0.03^{b}	5.72 ± 0.04^{a}
71	Ile Ile	C12H24N2O3	2.001969058	0.768648239	0.02448	4.05 ± 0.27^{b}	5.28 ± 0.01^{a}
72	His Tyr	C15H18N4O4	2.840939077	2.129705215	0.0408	4.69 ± 0.73^{a}	2.20 ± 0.01^{b}
73	Phe Val	C14H20N2O3	1.543983759	0.862251656	0.02607	4.55 ± 0.16^{b}	5.28 ± 0.01^{a}
74	Val Asp Tyr	C18H25N3O7	1.402150208	0.889009596	0.04862	4.90 ± 0.15^{b}	5.52 ± 0.12^{a}

(*continued on next page*)

Table 1 (*continued*)

No.	Metabolite	Formula	VIP_PLS-DA	FC (BS1/BS2)	P_value	BS1	BS2*
75	Tyr Met	C14H20N2O4S	1.914201678	0.745421245	0.01892	3.25 ± 0.02^{b}	4.36 ± 0.22^{a}
76	2-Phenylethyl 2-O-beta-D-xylopyranosyl-beta-*D*-glucopyranoside	C19H28O10	1.787450479	0.83172746	0.02807	4.83 ± 0.21^{b}	5.81 ± 0.09^{a}
77	Tuberoside	C34H56O8	1.944308182	0.781989609	0.007176	4.06 ± 0.10^{b}	5.19 ± 0.08^{a}
78	Leu Pro Ala	C14H25N3O4	1.316386011	0.897790055	0.006451	4.55 ± 0.04^{b}	5.06 ± 0.04^{a}
79	Val Ile Gly	C13H25N3O4	1.713712282	0.802466417	0.02496	3.64 ± 0.02^{b}	4.54 ± 0.20^{a}
80	Trp Gln	C16H20N4O4	1.299186659	0.896443309	0.04615	4.56 ± 0.15^{b}	5.08 ± 0.05^{a}
81	PD-160725 2-hydroxyethanesulfonate	C15H18N4O4	1.889580966	1.308137851	0.001673	4.51 ± 0.03^{a}	3.45 ± 0.05^{b}
82	Val Phe	C14H20N2O3	1.586424187	0.886026201	0.04412	6.08 ± 0.22^{b}	6.86 ± 0.08^{a}
83	Ala Ile	C9H18N2O3	1.128050859	0.915437128	0.01281	4.15 ± 0.02^{b}	4.54 ± 0.06^{a}
84	Val Met	C10H20N2O3S	1.333327898	0.903208363	0.0148	5.01 ± 0.08^{b}	5.54 ± 0.03^{a}
85	Gly Val Leu	C13H25N3O4	1.589872899	0.874691256	0.01051	5.31 ± 0.10^{b}	6.07 ± 0.04^{a}
86	Ala Tyr	C12H16N2O4	1.54603669	0.881956986	0.0106	5.37 ± 0.06^{b}	6.09 ± 0.08^{a}
87	Tyr Ala	C12H16N2O4	1.293934709	0.893478717	0.02093	4.26 ± 0.08^{b}	4.76 ± 0.06^{a}
88	Arg Leu	C12H25N5O3	2.138452256	0.717224185	0.000389	3.45 ± 0.02^{b}	4.81 ± 0.03^{a}
89	Ile Thr	C10H20N2O4	1.463414051	0.868592352	0.01377	4.26 ± 0.10^{b}	4.91 ± 0.03^{a}
90	His Leu Ala	C15H25N5O4	1.2906254	0.899554867	0.04617	4.64 ± 0.13^{b}	5.16 ± 0.09^{a}
91	Leu Gln	C11H21N3O4	1.454660607	0.881774313	0.01192	4.75 ± 0.09^{b}	5.38 ± 0.01^{a}
92	Tyr Gln	C14H19N3O5	1.056197692	0.933241973	0.02746	4.76 ± 0.07^{b}	5.10 ± 0.02^{a}
93	Lys Leu	C12H25N3O3	2.104782666	0.761818838	0.001672	4.22 ± 0.02^{b}	5.54 ± 0.07^{a}
94	Alanylmethionine	C8H16N2O3S	1.923204794	0.812189467	0.02968	4.90 ± 0.26^{b}	6.03 ± 0.10^{a}
95	*L*-Alanyl-l-Valine	C8H16N2O3	1.086247331	0.929384526	0.04099	4.81 ± 0.08^{b}	5.18 ± 0.06^{a}
96	Asn Val	C9H17N3O4	1.117940893	0.928251957	0.0349	4.98 ± 0.10^{b}	5.36 ± 0.02^{a}
97	Tyr Ser	C12H16N2O5	1.403672693	0.889407809	0.009287	4.76 ± 0.02^{b}	5.35 ± 0.07^{a}
98	Ser Val	C8H16N2O4	1.215178644	0.930685478	0.02668	6.06 ± 0.11^{b}	6.52 ± 0.01^{a}
99	Ile Arg	C12H25N5O3	2.052635198	0.754986312	0.000141	3.86 ± 0.02^{b}	5.11 ± 0.01^{a}
100	Guanosine monophosphate	C10H14N5O8P	1.527050661	0.873828532	0.04799	5.03 ± 0.22^{b}	5.76 ± 0.07^{a}
101	Cyanidin-3,5-diglucoside	C27H31O16+	1.255550802	0.931753689	0.02463	6.56 ± 0.11^{b}	7.04 ± 0.01^{a}
102	Met His	C11H18N4O3S	1.768929339	0.823407463	0.006247	4.36 ± 0.02^{b}	5.30 ± 0.10^{a}
103	Inosine 5'-Phosphate	C10H13N4O8P	1.56578304	0.858981639	0.0207	4.53 ± 0.10^{b}	5.28 ± 0.11^{a}
104	Guanosine 2′-monophosphate	C10H14N5O8P	2.958407848	0.5928125	0.000539	3.79 ± 0.02^{b}	6.39 ± 0.08^{a}
105	Thiodiacetic acid	C4H6O4S	1.897310268	0.784505079	0.009724	3.93 ± 0.02^{b}	5.02 ± 0.15^{a}
106	Artemidinol	C13H12O3	1.296007751	0.921633036	0.00193	5.89 ± 0.02^{b}	6.39 ± 0.02^{a}
107	Trehalose	C12H22O11	3.802402651	0.469385241	0.001238	3.8 ± 0.21^{b}	8.11 ± 0.01^{a}
108	2,3,4,5-Tetrahydro-2-pyridinecarboxylic acid	C6H9NO2	1.064935655	1.068443368	0.00487	5.29 ± 0.03^{a}	4.95 ± 0.01^{b}
109	4-Hydroxy-L-Proline	C5H9NO3	1.104980973	1.077268094	0.0494	5.28 ± 0.08^{a}	4.90 ± 0.09^{b}
110	*L*-Serine	C3H7NO3	1.367224806	1.131881003	0.01254	4.83 ± 0.01^{a}	4.26 ± 0.08^{b}
111	*L*-2,4-diaminobutyric acid	C4H10N2O2	1.710951851	1.245814732	0.01305	4.46 ± 0.06^{a}	3.58 ± 0.13^{b}
112	*L*-Alanine	C3H7NO2	1.031383065	1.053344482	0.01021	6.29 ± 0.04^{a}	5.97 ± 0.02^{b}
113	Methyldopa	C10H13NO4	1.455749938	0.882806892	0.03503	4.91 ± 0.17^{b}	5.57 ± 0.03^{a}
114	Deoxyhypusine	C10H23N3O2	1.157003192	0.91890292	0.03664	4.65 ± 0.10^{b}	5.06 ± 0.05^{a}
115	(3*S*)-3,7-Diaminoheptanoic Acid	C7H16N2O2	1.299995429	1.107067287	0.007422	5.23 ± 0.03^{a}	4.72 ± 0.05^{b}
116	Hypusine	C10H23N3O3	1.115684989	0.926404384	0.01727	4.73 ± 0.02^{b}	5.10 ± 0.06^{a}
117	*S*-Adenosylhomocysteine	C14H20N6O5S	1.135006241	0.94298441	0.00109	6.35 ± 0.01^{b}	6.73 ± 0.02^{a}
118	Arg Phe	C15H23N5O3	1.729694154	0.85256514	0.02287	5.26 ± 0.19^{b}	6.17 ± 0.04^{a}
119	*D*-Tyrosine	C9H11NO3	1.100749149	0.928176796	0.007577	4.70 ± 0.02^{b}	5.06 ± 0.04^{a}
120	Lactose	C12H22O11	3.357229292	0.523586246	0.000023	3.68 ± 0.02^{b}	7.03 ± 0.01^{a}

* BS1 and BS2 represent the nonflavored and flavored treatments. The different letters in the same row indicated significant differences ($P < 0.05$).

the volatile flavors. Correlation coefficients were deemed statistically significant if their value exceeded 0.2 and the corresponding $P < 0.05$. The TBtools-II (v2.096) software was used to generate heatmaps displaying the correlation coefficients between lipid compounds and flavors that have a positive correlation. Furthermore, the relationship between lipids and lipid-like compounds and volatile flavors was analyzed using partial least-squares regression (PLSR) with the assistance of Unscrambler X 10.4 software.

Results and discussion

Nonvolatile metabolite profile

The total ion chromatogram of the samples was acquired in negative and positive ion scanning modes (Fig. S1). Under these detection conditions (Fig. S1), the distribution and peak shape were quite stable. A total of 1791 metabolites were qualified using biochemical databases after baseline screening, peak qualification, integration, and correction of retention time. Among these metabolites, 1183 were qualified in positive ion mode and 608 in negative ion mode.

The metabolites were separated into 15 groups (Fig. 1A), including lipids and lipid-like molecules (33.87 %), organoheterocyclic compounds (13.09 %), organic acids and derivatives (30.97 %); organic oxygen compounds (7.49 %); benzenoids (4.32 %); nucleosides, nucleotides, and analogs (4.39 %); organic nitrogen compounds (2.09 %); phenylpropanoids and polyketides (2.50 %); alkaloids and derivatives (0.61 %); hydrocarbons (0.20 %); homogeneous nonmetal compounds (0.13 %); hydrocarbons derivatives (0.07 %); lignans, neolignans, and related compounds (0.07 %); organosulfur compounds (0.07 %); and not available (0.13 %). The superclass category included three different kinds of metabolites constituting 77.93 %, including lipids and lipid-like compounds (502 species, 33.87 %); organic acids and derivatives (459 species, 30.97 %); and organoheterocyclic compounds (194, 13.09 %; Fig. 1A). Setyabrata et al. (2022) identified 1405 metabolite characteristics in cull beef loins subjected to different dry-aging procedures. Sixty metabolites were selected for subsequent analysis upon the identification of a significant influence of the aging treatment on these metabolites ($P < 0.05$, FDR < 0.05). Li et al. (2022) reported that the two most abundant classes of metabolites in cured ducks were lipids and lipid-like compounds (476 species) and organic acids and derivatives (190 species).

Lipids and lipid-like compounds

The most prevalent metabolites in raw beef are lipids and lipid-like compounds, including fatty acyls (222 species, 14.98 %), glycerophospholipids (145 species, 9.78 %), prenol lipids (90 species, 6.07 %),

Table 2
106 Differential metabolites between BS1 and BS2 at 3 months of frozen storage.*

No.	Metabolite	Formula	VIP_PLS-DA	FC (BS1/BS2)	P_value	BS1	BS2
1	Spermine	C10H26N4	1.816888196	0.894305373	0.0008144	6.10 ± 0.02^{b}	6.83 ± 0.01^{a}
2	3-Isopropenylpentanedioic acid	C8H12O4	1.02414222	1.053312514	0.03974	4.72 ± 0.05^{a}	4.48 ± 0.05^{b}
3	Val Lys	C11H23N3O3	1.336514599	1.069611307	0.0106	6.05 ± 0.05^{a}	5.65 ± 0.01^{b}
4	Geniposidic acid	C16H22O10	2.444754115	1.299497028	0.002822	5.68 ± 0.05^{a}	4.37 ± 0.08^{b}
5	Cis-Acetylacrylate	C5H6O3	2.11961961	0.811796144	0.004141	4.25 ± 0.07^{b}	5.23 ± 0.05^{a}
6	Furfural	C5H4O2	1.985227287	0.85183912	0.0008104	4.95 ± 0.02^{b}	5.81 ± 0.03^{a}
7	Kaempferol 3-neohesperidoside-7-(2″-p-coumaryllaminaribioside)	C48H56O27	1.710104668	0.90510083	0.001841	6.10 ± 0.03^{b}	6.74 ± 0.01^{a}
8	L-Carnitine	C7H15NO3	1.135336507	1.036830074	0.03154	8.16 ± 0.04^{a}	7.87 ± 0.06^{b}
9	2-*O*-Alpha-D-Mannopyranosyl-D-Mannopyranose	C12H22O11	1.34853276	0.918849206	0.02942	4.63 ± 0.03^{b}	5.04 ± 0.09^{a}
10	Melezitose	C18H32O16	1.877937901	0.860519248	0.009777	4.80 ± 0.04^{b}	5.58 ± 0.10^{a}
11	Ile Asn	C10H19N3O4	1.554292215	0.912871938	0.005726	5.55 ± 0.03^{b}	6.08 ± 0.05^{a}
12	Ile Ser	C9H18N2O4	1.086410376	0.952945402	0.01816	5.30 ± 0.05^{b}	5.56 ± 0.01^{a}
13	Phosphoribosyl formamidocarboxamide	C10H15N4O9P	1.012239597	0.962999507	0.006985	5.85 ± 0.02^{b}	6.08 ± 0.02^{a}
14	Ile Gln	C11H21N3O4	1.245247683	0.936092291	0.02865	5.11 ± 0.08^{b}	5.46 ± 0.01^{a}
15	1-Methylhypoxanthine	C6H6N4O	1.720256241	1.195268044	0.007699	3.99 ± 0.05^{a}	3.33 ± 0.06^{b}
16	Kainic acid	C10H15NO4	1.117444657	1.050319052	0.01084	5.76 ± 0.03^{a}	5.48 ± 0.03^{b}
17	2'-Fluorothymidine	C10H13FN2O5	1.363949251	0.928571429	0.04737	5.55 ± 0.10^{b}	5.97 ± 0.09^{a}
18	Tetraethylene Glycol Monododecyl Ether	C20H42O5	1.464855112	1.095191556	0.03709	5.60 ± 0.11^{a}	5.11 ± 0.08^{b}
19	17-Hydroxymethylethisterone	C22H30O3	1.042381106	0.952586207	0.022	4.86 ± 0.05^{b}	5.10 ± 0.01^{a}
20	Histidyltyrosine	C15H18N4O4	1.631251981	0.862572422	0.01917	3.72 ± 0.05^{b}	4.31 ± 0.11^{a}
21	Phenethylamine glucuronide	C14H19NO6	1.068263139	1.046727239	0.007834	5.64 ± 0.02^{a}	5.39 ± 0.03^{b}
22	Salicyl-6-hydroxy-2-cyclohexene-on-oyl	C14H14O5	1.196960815	1.062812563	0.0001214	5.31 ± 0.01^{a}	4.99 ± 0.01^{b}
23	Met Val	C10H20N2O3S	1.895658632	0.851189379	0.02646	4.61 ± 0.01^{b}	5.42 ± 0.18^{a}
24	3'-Amino-3′-deoxythimidine	C10H15N3O4	2.222723981	1.252729754	0.02807	5.50 ± 0.07^{a}	4.39 ± 0.25^{b}
25	Gln Asn Ile	C15H27N5O6	1.442379167	0.906753043	0.04238	4.61 ± 0.14^{b}	5.09 ± 0.02^{a}
26	Trp Glu	C16H19N3O5	1.216754607	0.936207569	0.009885	4.79 ± 0.01^{b}	5.12 ± 0.04^{a}
27	Glu Phe Gly	C16H21N3O6	2.109498433	0.812640239	0.03	4.34 ± 0.16^{b}	5.34 ± 0.19^{a}
28	*N*-butyryl-L-Homocysteine thiolactone	C8H13NO2S	1.232027165	1.12647619	0.002972	2.95 ± 0.02^{a}	2.62 ± 0.01^{b}
29	Leucyl-Tyrosine	C15H22N2O4	1.319138967	0.927146084	0.01697	4.92 ± 0.04^{b}	5.31 ± 0.05^{a}
30	Alanyl-dl-phenylalanine	C12H16N2O3	1.27822953	0.934805654	0.0326	5.29 ± 0.09^{b}	5.65 ± 0.02^{a}
31	2-*O*-(6-Phospho-alpha-mannosyl)-D-glycerate	C9H17O12P	2.490349052	0.815675088	0.00107	6.00 ± 0.05^{b}	7.36 ± 0.03^{a}
32	PG(i-14:0/i-13:0)	C33H65O10P	1.393041608	0.916457165	0.01968	4.73 ± 0.08^{b}	5.17 ± 0.01^{a}
33	2-Hydroxydecanedioic acid	C10H18O5	1.686900691	1.149221557	0.003119	4.79 ± 0.04^{a}	4.17 ± 0.02^{b}
34	CHEBI:69439	C10H16N2O2	1.376335244	1.100230947	0.0482	4.76 ± 0.02^{a}	4.33 ± 0.13^{b}
35	3'-Amino-3′-deoxythimidine glucuronide	C16H23N3O10	2.153795718	0.807406029	0.02011	4.33 ± 0.16^{b}	5.37 ± 0.13^{a}
36	Leucylproline	C11H20N2O3	1.046193979	1.051028979	0.01573	5.00 ± 0.03^{a}	4.76 ± 0.02^{b}
37	Kynuramine	C9H12N2O	1.372834449	1.089808917	0.02612	5.13 ± 0.08^{a}	4.71 ± 0.05^{b}

(*continued on next page*)

Table 2 (*continued*)

No.	Metabolite	Formula	VIP_PLS-DA	FC (BS1/BS2)	P_value	BS1	BS2
38	2-Hydroxy-p-mentha-1,8-dien-6-one	C10H14O2	1.65049408	1.200384123	0.04861	3.75 ± 0.19[a]	3.12 ± 0.04[b]
39	6-Hydroxymelatonin glucuronide	C19H24N2O9	1.41130259	0.906339468	0.04905	4.43 ± 0.01[b]	4.88 ± 0.14[a]
40	Kuwanon F	C25H26O6	1.763979965	0.867451283	0.01163	4.49 ± 0.08[b]	5.18 ± 0.06[a]
41	Caffeoyl tyrosine	C18H17NO6	1.564530313	0.887770086	0.0001981	4.23 ± 0.01[b]	4.76 ± 0.01[a]
42	*P*-Hydroxyphenyl-phenylhydantoin	C15H12N2O3	1.529989705	1.15957121	0.01813	3.78 ± 0.10[a]	3.26 ± 0.01[b]
43	Prostaglandin PGE2 glyceryl ester	C23H38O7	1.85663601	0.833223467	0.006673	3.79 ± 0.08[b]	4.55 ± 0.02[a]
44	3-Pyridinamine	C5H6N2	1.468998077	1.085396484	0.009943	6.04 ± 0.05[a]	5.57 ± 0.03[b]
45	*D*-Pipecolic acid	C6H11NO2	1.234533227	1.0558965	0.01222	6.36 ± 0.03[a]	6.02 ± 0.04[b]
46	*O*-Arachidonoyl Glycidol	C23H36O3	1.441886932	1.114815743	0.009258	4.44 ± 0.05[a]	3.98 ± 0.03[b]
47	Choline Phosphate	C5H14NO4P	1.105338254	1.058342078	0.03965	5.04 ± 0.06[a]	4.76 ± 0.05[b]
48	LysoPC(22:4(7Z,10Z,13Z,16Z)/0:0)	C30H54NO7P	1.708533407	1.168016723	0.007859	4.46 ± 0.05[a]	3.82 ± 0.06[b]
49	PC(P-16:0/2:0)	C26H52NO7P	1.306710246	1.067522999	0.03942	6.14 ± 0.03[a]	5.76 ± 0.10[b]
50	Docosa-4,7,10,13,16-pentaenoyl carnitine	C29H47NO4	1.002209805	1.043896804	0.03675	5.42 ± 0.03[a]	5.19 ± 0.05[b]
51	Petasinine	C13H21NO3	1.374346283	1.077322455	0.009127	5.80 ± 0.02[a]	5.39 ± 0.05[b]
52	Phe Lys	C15H23N3O3	1.468066254	0.909241532	0.04436	4.93 ± 0.11[b]	5.43 ± 0.10[a]
53	All-trans-Heptaprenyl diphosphate	C35H60O7P2	3.739242994	0.321763807	0.01686	1.47 ± 0.03[b]	4.58 ± 0.57[a]
54	LysoPC(0:0/18:1(9Z))	C26H52NO7P	1.440261687	1.073767886	0.02448	6.75 ± 0.10[a]	6.28 ± 0.02[b]
55	Docosatrienoic acid	C22H38O2	1.096102562	0.945106908	0.01816	4.59 ± 0.05[b]	4.86 ± 0.02[a]
56	PC(16:1(9Z)/16:0)	C40H78NO8P	1.896982068	1.185424354	0.02231	5.14 ± 0.13[a]	4.33 ± 0.10[b]
57	9,12-Octadecadiynoic Acid	C18H28O2	1.422297249	0.908595642	0.02364	4.50 ± 0.07[b]	4.95 ± 0.06[a]
58	Auxin a	C18H32O5	1.276619858	0.919723781	0.04429	4.26 ± 0.03[b]	4.63 ± 0.11[a]
59	Gln Ala Met	C13H24N4O5S	2.556836144	1.600502513	0.003609	3.82 ± 0.12[a]	2.38 ± 0.01[b]
60	(+/−)-2-(2-Furanyl)pyrrolidine	C8H11NO	1.728512739	0.826928037	0.02774	3.20 ± 0.01[b]	3.87 ± 0.16[a]
61	20-COOH-leukotriene E4	C23H35NO7S	1.778247101	0.861520096	0.006573	4.33 ± 0.02[b]	5.02 ± 0.07[a]
62	*P*-Coumaroyl 3-hydroxytyrosine	C18H17NO6	1.436605751	0.906186406	0.02012	4.45 ± 0.02[b]	4.91 ± 0.09[a]
63	Cyclo(proline-leucine)	C11H18N2O2	1.162068057	1.064233888	0.01929	4.98 ± 0.01[a]	4.68 ± 0.05[b]
64	PE(20:5(5Z,8Z,11Z,14Z,17Z)/18:4(6Z,9Z,12Z,15Z))	C43H68NO8P	2.33813596	0.755234804	0.007181	3.71 ± 0.03[b]	4.91 ± 0.14[a]
65	(3*S*)-3,6-Diaminohexanoate	C6H14N2O2	1.256897962	0.923159476	0.03502	4.30 ± 0.03[b]	4.65 ± 0.09[a]
66	Ile Leu	C12H24N2O3	1.195455692	0.950170226	0.03052	6.13 ± 0.07[b]	6.46 ± 0.02[a]
67	Pseudoecgonine	C9H15NO3	1.278605395	1.097605893	0.03822	4.17 ± 0.06[a]	3.80 ± 0.08[b]
68	Tyr Leu	C15H22N2O4	1.414397508	0.92256296	0.03222	5.38 ± 0.08[b]	5.83 ± 0.08[a]
69	Asn Trp	C15H18N4O4	1.518508933	0.904215976	0.02723	4.89 ± 0.09[b]	5.40 ± 0.07[a]
70	Ile Ile	C12H24N2O3	1.631346064	0.89110201	0.005436	4.78 ± 0.04[b]	5.37 ± 0.04[a]
71	1-cyclohexyl-3-[[1-(hydroxymethyl)cyclopropyl]methyl]urea	C12H22N2O2	1.569697875	1.105882353	0.003501	5.64 ± 0.04[a]	5.10 ± 0.01[b]
72	2-Octenedioic acid	C8H12O4	1.129853964	1.066494361	0.01464	4.53 ± 0.01[a]	4.25 ± 0.04[b]
73	2-Phenylethyl 2-O-beta-D-xylopyranosyl-beta-D-glucopyranoside	C19H28O10	1.326007075	0.934673367	0.01439	5.57 ± 0.01[b]	5.96 ± 0.06[a]
74	Val Ile Gly	C13H25N3O4	2.355813082	0.755795981	0.04032	3.91 ± 0.33[b]	5.17 ± 0.16[a]
75	PD-160725 2-hydroxyethanesulfonate	C15H18N4O4	2.49113941	1.396491228	0.0005092	4.77 ± 0.04[a]	3.41 ± 0.01[b]

(*continued on next page*)

Table 2 (*continued*)

No.	Metabolite	Formula	VIP_PLS-DA	FC (BS1/BS2)	P_value	BS1	BS2
76	2-(Methylamino)benzoic acid	C8H9NO2	1.416291485	0.866727383	0.002411	2.85 ± 0.02^{b}	3.29 ± 0.02^{a}
77	5-Hydroxyvalproic acid	C8H16O3	1.768444935	1.180184805	0.02869	4.59 ± 0.03^{a}	3.89 ± 0.16^{b}
78	Luteolinidin 3-O-glucoside	C21H21O10+	1.757927755	1.179151388	0.01301	4.50 ± 0.11^{a}	3.81 ± 0.01^{b}
79	Gly Val Leu	C13H25N3O4	1.354011864	0.934541954	0.0189	5.82 ± 0.01^{b}	6.23 ± 0.07^{a}
80	Gibberellin A53	C20H28O5	1.141606681	0.909904351	0.02422	2.94 ± 0.02^{b}	3.24 ± 0.06^{a}
81	Hydroxytyrosol 4'-O-glucoside	C14H20O8	1.310793091	0.873057851	0.02159	2.64 ± 0.08^{b}	3.02 ± 0.01^{a}
82	Ala Tyr	C12H16N2O4	1.139903845	0.952102614	0.03738	5.86 ± 0.06^{b}	6.15 ± 0.05^{a}
83	Isopropyl beta-D-glucoside	C9H18O6	1.091940115	1.045603731	0.01258	6.05 ± 0.01^{a}	5.78 ± 0.04^{b}
84	Epidermin	C11H19NO6	1.811502569	1.160122164	0.02446	5.31 ± 0.11^{a}	4.58 ± 0.12^{b}
85	Neotussilagine	C10H17NO3	1.015532085	1.051264679	0.007222	4.65 ± 0.02^{a}	4.42 ± 0.01^{b}
86	Leu Gln	C11H21N3O4	1.283099127	0.930094567	0.0453	5.01 ± 0.11^{b}	5.39 ± 0.02^{a}
87	*S*-(1,2-Dicarboxyethyl)glutathione	C14H21N3O10S	1.556453067	0.896981132	0.03315	4.75 ± 0.06^{b}	5.30 ± 0.13^{a}
88	Tyr Asn	C13H17N3O5	1.028650677	0.957558245	0.01277	5.30 ± 0.01^{b}	5.53 ± 0.04^{a}
89	Ile Arg	C12H25N5O3	1.812298541	0.856601516	0.002211	4.29 ± 0.04^{b}	5.01 ± 0.02^{a}
90	Guanosine monophosphate	C10H14N5O8P	1.116479152	0.952939148	0.001143	5.52 ± 0.01^{b}	5.80 ± 0.01^{a}
91	7-Deaza-2′-deoxyguanosine	C11H14N4O4	1.328694672	1.085763293	0.03577	5.06 ± 0.11^{a}	4.66 ± 0.01^{b}
92	5-Aminoimidazole-4-carboxamide-1-beta-D-ribofuranosyl 5′-monophosphate	C9H15N4O8P	1.440646136	0.918363854	0.04921	5.36 ± 0.09^{b}	5.84 ± 0.12^{a}
93	Guanosine 2′-monophosphate	C10H14N5O8P	3.453594824	0.596377148	0.0001002	3.85 ± 0.04^{b}	6.45 ± 0.01^{a}
94	Artemidinol	C13H12O3	1.416617493	0.929978118	0.02129	5.94 ± 0.03^{b}	6.39 ± 0.08^{a}
95	Trehalose	C12H22O11	4.137911557	0.530295567	0.02035	4.30 ± 0.78^{b}	8.12 ± 0.04^{a}
96	4-Hydroxy-L-Proline	C5H9NO3	1.012689694	1.04696243	0.04618	5.23 ± 0.04^{a}	5.00 ± 0.06^{b}
97	3-(1-Pyrazolyl)-Alanine	C6H9N3O2	1.032762495	1.037661519	0.0272	6.58 ± 0.03^{a}	6.34 ± 0.05^{b}
98	*P*-Toluenesulfonyl fluoride	C7H7FO2S	1.902877369	0.846629213	0.03367	4.52 ± 0.04^{b}	5.34 ± 0.21^{a}
99	Deoxyhypusine	C10H23N3O2	1.343348451	0.920995457	0.01446	4.66 ± 0.05^{b}	5.06 ± 0.04^{a}
100	(3*S*)-3,7-Diaminoheptanoic Acid	C7H16N2O2	1.520027836	1.106683534	0.002698	5.24 ± 0.04^{a}	4.74 ± 0.01^{b}
101	*N*-Jasmonoylisoleucine	C18H29NO4	1.355760862	1.083215226	0.02364	5.34 ± 0.05^{a}	4.93 ± 0.07^{b}
102	Benzoquinoneacetic acid	C8H6O4	1.371904326	1.090014654	0.04568	5.20 ± 0.09^{a}	4.77 ± 0.09^{b}
103	Arg Phe	C15H23N5O3	1.554555878	0.914733643	0.00901	5.71 ± 0.02^{b}	6.25 ± 0.06^{a}
104	4-Aminohippuric acid	C9H10N2O3	1.211652051	1.056271186	0.03574	6.23 ± 0.08^{a}	5.89 ± 0.02^{b}
105	*D*-TYROSINE	C9H11NO3	1.03824915	0.952675295	0.03945	4.93 ± 0.06^{b}	5.17 ± 0.03^{a}
106	Lactose	C12H22O11	3.896378213	0.530019824	0.0001262	3.74 ± 0.03^{b}	7.06 ± 0.04^{a}

* BS1 and BS2 represent the nonflavored and flavored treatments. The different letters in the same row indicated significant differences ($P < 0.05$).

and steroids and steroid derivatives (32 species, 2.16 %), sphingolipids (8 species, 0.536 %), glycerolipids (4 species, 0.268 %), and sacchrolipids (1 species, 0.067 %; Fig. 1B). The extensive categorization and characterization of the lipids and lipid-like compounds in this study are crucial to research on the effects of flavoring substances and frozen storage on the complicated metabolic pathways of lipid molecules. Fatty acyls are the predominant category of lipids and lipid-like compounds in raw beef meat, which include fatty acids and conjugates (96 species, 6.48 %), fatty acid esters (60 species, 4.05 %), fatty acyl glycosides (18 species, 1.21 %), linoleic acids and derivatives (15 species, 1.01 %), eicosanoids (16 species, 1.08 %), fatty alcohols (11 species, 0.74 %), and fatty alcohols esters (2 species, 0.13 %), as shown in Fig. 1C. Li et al. (2022) reported that the majority of the fatty acyls found in duck meat belong to five subclasses: fatty acid esters; fatty acyl glycosides; eicosanoids; fatty acids and conjugates; and linoleic acids and derivatives. Fatty acids play a significant role in the flavor development and rancidity of traditional meat products. The majority of flavor compounds were primarily obtained through the auto-oxidation or enzymatic oxidation of unsaturated fatty acids, specifically oleic, linoleic, and linolenic acids, which are the most prevalent in beef and constitute

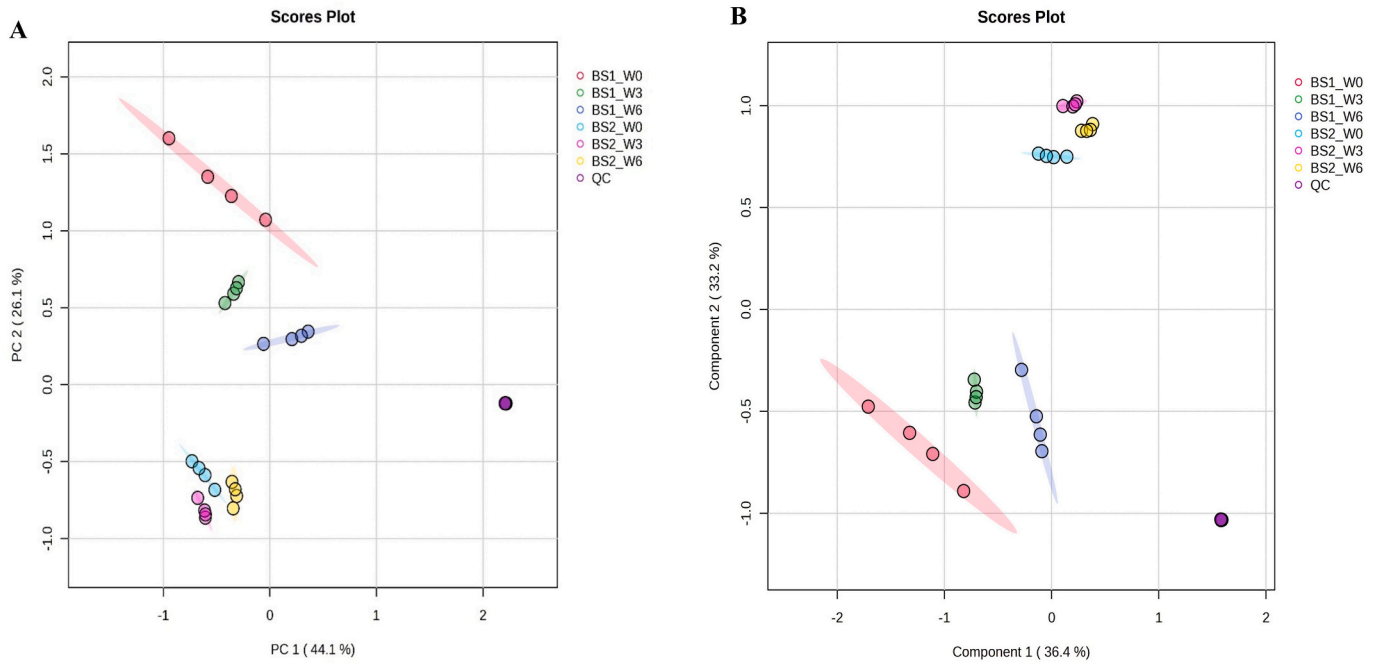

Fig. 2. Effect of flavoring substances on the metabolites; A. unsupervised PCA of metabolites from the BS1 and BS2 samples at different times of frozen storage; B. supervised PLS–DA of the metabolites from the BS1 and BS2 samples at different times of frozen storage.

4.5 %, 0.48 %, and 0.14 % of the overall percentage, respectively (Al-Dalali et al., 2022a). Al-Dalali et al. (2021) reported that adding different seasoning substances improves the aroma profile and serves as a standard for marinated meat products.

The second predominant group is composed of glycerophospholipids, including phosphatidylcholines (PCs; 74 species, 4.99 %), phosphatidylethanolamines (50 species, 3.37 %), glycerophosphates (7 species, 0.47 %), phosphatidylglycerols (7 species, 0.47 %), phosphatidylinositols (5 species, 0.33 %), phosphosphingolipids (5 species, 0.33 %), and phosphatidylserines (2 species, 0.13 %). The third largest group is composed prenol lipids, which include terpene glycosides (11 species, 0.74 %), diterpenoids (11 species, 0.74 %), monoterpenoids (21 species, 1.42 %), and sesquiterpenoids (23 species, 1.55 %; Fig. 1C). The flavor development and rancidity of traditional meat products are greatly influenced by phospholipids (Li et al., 2022). Gu et al. (2021) stated that the primary components of cell membranes are phospholipids. Hence, the elevated concentration of phospholipids, including long-chain PUFAs, may be associated with the enhanced plateau adaptation observed in the cattle–yak hybrid and yak compared with cattle. Liu et al. (2020) demonstrated that the muscle composition of phospholipids in Atlantic salmon exhibited sensitivity to a decrease in temperature; they suggested increasing the phospholipid PUFA content to compensate for the rearrangement of biological membranes to promote homeostasis.

Organic acids and derivatives

The second prevalent group of metabolites is composed of organic acids and derivatives (Fig. 1A), which are primarily composed of carboxylic acids and derivatives (426 species, 28.74 %), hydroxy acids and derivatives (11 species, 0.74 %), keto acids and derivatives (7 species, 0.46), peptidomimetics (10 species, 0.67 %), organic sulfuric acids and derivatives (3 species, 0.19), and carboximidic acids and derivatives (1 species, 0.06 %; .Fig. 1B). In addition, 411 amino acids, peptides, and analogs were detected in the carboxylic acids and their derivatives (. Fig. 1C). Several studies focused on analyzing the essential amino acids and peptidomics profile of processed beef; however, the effects of flavoring substances and frozen storage on amino acids, peptides, analogs molecules in raw beef have not been explored. Notably, many dipeptides have either aspartyl or glutamyl residues, such as asparaginyl–valine. Thus, beef has umami taste and sensory qualities. For humans, only L-aspartate and *L*-glutamate have an umami taste. The umami taste is frequently present in small peptides that include at least one of the aforementioned two amino acids (Etiévant et al., 2016; Li et al., 2022). In addition, inosine 5′-monophosphate (IMP) and guanosine monophosphate (GMP) are the primary umami components of meat from cattle, poultry, livestock, and fish, having crucial functions in the development of meat flavor (Ramalingam et al., 2019). In this study, IMP was found at 4.53 and 5.28 in BS1 and BS2, respectively, at 0 months (.Table 1), whereas GMP was determined at 5.03 (BS1) and 5.76 (BS2) at 0 months and 5.52 (BS1) and 5.80 (BS2) at 3 months (Tables 1 and 2). Various studies have demonstrated the strong correlations among IMP, the taste of meat, and the level of satisfaction with fish meat (Resconi et al., 2013).

Organoheterocyclic compounds

The third most prevalent group of metabolites is organoheterocyclic compounds (Fig. 1A), which are mainly composed of indoles and derivatives (29 species, 1.96 %), pyridines and derivatives (24 species, 1.62 %), imidazopyrimidines (19 species, 1.28 %), lactones (17 species, 1.15 %), diazines (16 species, 1.08 %), and azoles (11 species, 0.74 %; Fig. 1B). The primary constituents of organoheterocyclic compounds are indoles, pyridines, and their derivatives.

Influences of flavoring substances and frozen storage on the metabolite profiles

Nonflavored (BS1) and flavored (BS2) metabolites were screened and differentiated through unsupervised PCA and supervised PLS–DA. The findings of PCA revealed that the BS1 and BS2 samples were positioned on opposite areas of the negative and positive half axes of PCA without any shared overlap (Fig. 2A). The PCA score plot indicated that PC1 accounted for 44.1 % of the variance and PC2 for 26.1 %. PLS–DA was consistent with PCA (Fig. 2B), suggesting that flavoring substances significantly affected the metabolites. PLS–DA plots indicated that components 1 and 2 accounted for 36.4 % and 33.2 % of the total variance, respectively, indicating that supervised PLS–DA explained

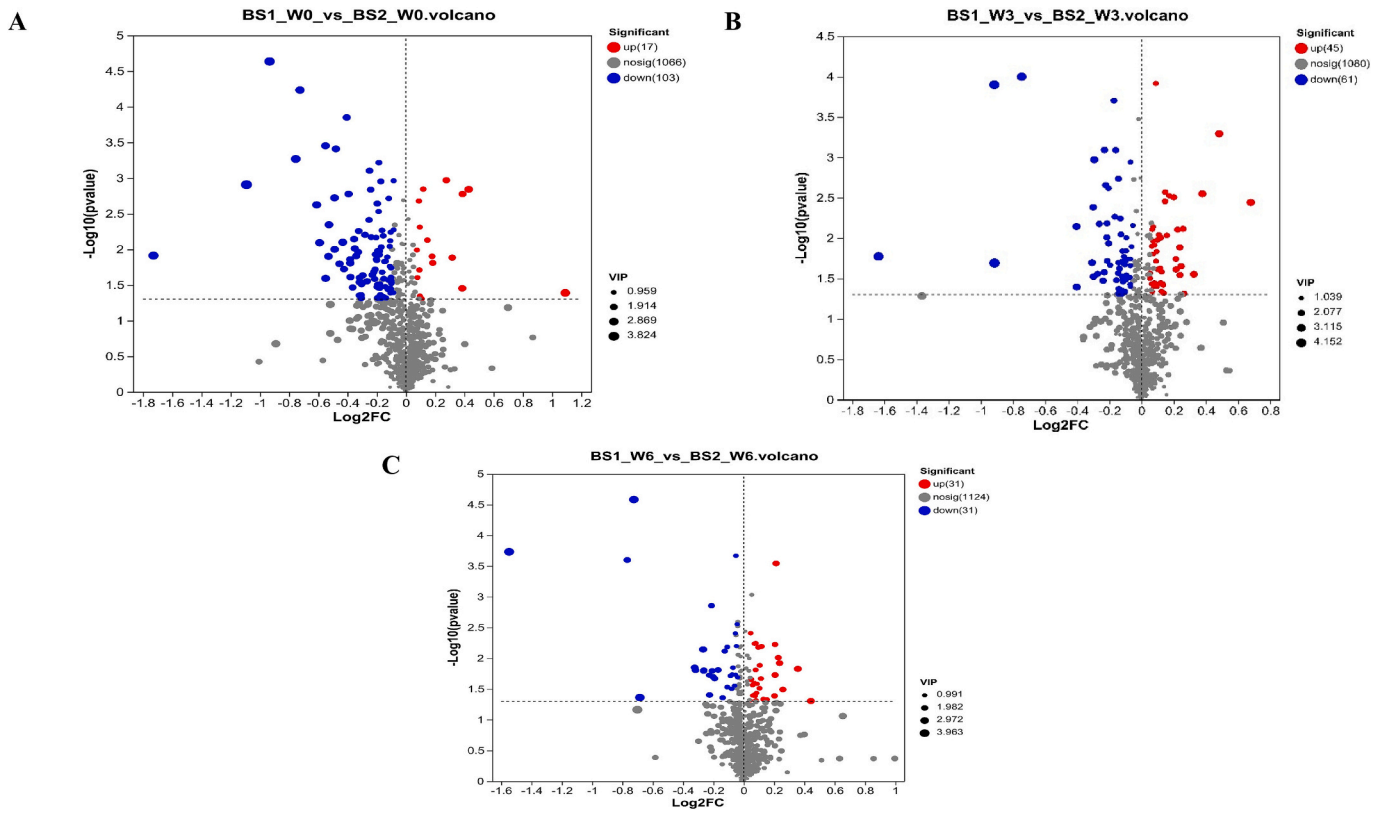

Fig. 3. Differential metabolite identification between the BS1 and BS2 samples. Volcano plot of identical biomarkers during frozen storage: A, 0 months; B, 3 months; C, 6 months. Metabolites that were up- or down-regulated are shown by red or blue dots, respectively. Gray represents metabolites that did not differ from each other. (For interpretation of the references to color in this figure legend, the reader is referred to the web version of this article.)

69.6 % of the total variance.

The differential metabolites were filtered by different statistical analysis techniques, including the VIP and volcano plot, and the effects of flavoring substances on metabolites were elucidated. A *P* value of <0.05, VIP of >1.0, and fold change (FC) > 1 or < 1 were to be used to characterize metabolite differences between the BS1 and BS2 samples. The volcano plots demonstrate differential metabolite visualization between BS1 and BS2 at different frozen storage times, as shown in Figs. 3A, B, and C. In a statistical test, the combination of statistical significance measures and change amplitudes is shown by a volcano plot, which is a type of scatter map. It can quickly and accurately identify data points with a high statistical significance level and significant changes in abundance. The FC values are shown along the horizontal axis. FC is defined as "the ratio of the mean abundance of a compound in one group of samples to the mean abundance in another" (Li et al., 2022). Compounds with *P* values lower than 0.05 are shown along the horizontal axis. A total of 1186 differential metabolites in the comparison between BS1 and BS2 were subjected to differential metabolite analyses, and only 920, 793, and 576 metabolites met the differential screening conditions at 0, 3, and 6 months of frozen storage, respectively. At 0 months of frozen storage, 120 different metabolites were identified after 920 metabolites in the BS1 and BS2 samples were screened (Fig. 3A). The details of 120 metabolites at 0 months of frozen storage are listed in Table 1. In Fig. 3A, the red dots represent 17 metabolites that were up-regulated ($FC_{(BS1\_W0/BS2\_W0)} > 1$), the blue dots represent 103 metabolites that were down-regulated ($FC_{(BS1\_W0/BS2\_W0)} < 1$), and the gray dots represent 800 metabolites with no significant difference. Moreover, 793 metabolites were screened in BS1 and BS2 samples at 3 months of frozen storage; among them, 106 metabolites were characterized as differential metabolites. The details of 106 metabolites are listed in Table 2. Fig. 3B shows that 45 out of 106 metabolites were up-regulated ($FC_{(BS1\_W3/BS2\_W3)} > 1$), 61 metabolites were down-regulated ($FC_{(BS1\_W3/BS2\_W3)} < 1$), and 687 metabolites showed no difference. At 6 months of frozen storage, 62 metabolites were differentially screened from the 576 metabolites in BS1 and BS2. The details of the screened metabolites are listed in Table 3. Fig. 3C shows that 31 out of the 62 metabolites were up-regulated ($FC_{(BS1\_W6/BS2\_W6)} > 1$), 31 metabolites were down-regulated ($FC_{(BS1\_W6/BS2\_W6)} < 1$), and 483 metabolites showed no difference. This result suggested the significant effect of frozen storage on the metabolite profiles of beef. The metabolites were reduced along with frozen storage from 920 metabolites at 0 months to 576 metabolites at 6 months. The reduction in the differential metabolites during frozen storage can be ascribed to the actions of these metabolites as precursors for the formation of flavor, taste, and other functional components. Take amino acids, peptides, and analogues as an example. As the frozen storage periods increased, their levels decreased. This suggests that these metabolites are degrading due to continuous oxidation as a result of the combination effect of frozen and added salt. These metabolites contribute to the overall quality of raw beef by creating other metabolites that improve its flavor and aroma. Meanwhile, frozen storage reduced the levels of organoheterocyclic compounds, which improved the safety and quality of raw beef meat. This is significant since these metabolites can affect the quality of raw beef meat if they accumulate. In contrast, there was an increase in organic nitrogen compounds, lipids and lipid-like molecules, carbohydrates and carbohydrate conjugates, organic oxygen compounds, and organic nitrogen compounds with frozen storage. This suggests that pyrolysis and lipolysis are still occurring, producing metabolites that improve the raw beef's quality. Tamura et al. (2022) reported an increase in free fatty acid (FFA) levels, likely due to lipid oxidation and lipolysis in pork during refrigerated storage (Monin et al., 2003). The data indicated that lipids and lipid-like molecules accumulated during frozen storage and were released as FFAs. Furthermore, carbohydrates and carbohydrate conjugates increased during frozen storage, particularly in the BS1 sample.

Table 3
62 Differential metabolites between BS1 and BS2 at 6 months of frozen storage.*

No.	Metabolite	Formula	VIP_PLS-DA	FC (BS1/BS2)	P_value	BS1	BS2
1	Asp Val Lys	C15H28N4O6	1.198805811	0.952440328	0.01424	5.34 ± 0.07[b]	5.61 ± 0.04[a]
2	Spermine	C10H26N4	2.010846392	0.889654162	0.01552	6.07 ± 0.05[b]	6.80 ± 0.12[a]
3	Val Lys	C11H23N3O3	1.260913975	1.053146853	0.04103	6.02 ± 0.08[a]	5.72 ± 0.01[b]
4	Geniposidic acid	C16H22O10	2.062823208	1.15970516	0.0002867	5.66 ± 0.01[a]	4.88 ± 0.01[b]
5	Asparaginyl-Valine	C9H17N3O4	1.036586452	1.031894637	0.02268	6.50 ± 0.04[a]	6.30 ± 0.01[b]
6	Cis-Acetylacrylate	C5H6O3	2.34261081	0.802129719	0.01555	4.14 ± 0.15[b]	5.16 ± 0.09[a]
7	Furfural	C5H4O2	1.948168823	0.875481611	0.02136	4.99 ± 0.02[b]	5.70 ± 0.14[a]
8	L-Carnitine	C7H15NO3	1.17600037	1.032335785	0.003906	8.14 ± 0.02[a]	7.88 ± 0.01[b]
9	Melezitose	C18H32O16	1.539714249	0.916951729	0.007657	4.80 ± 0.01[b]	5.26 ± 0.05[a]
10	1-Methylhistidine	C7H11N3O2	1.144135175	1.060334383	0.03668	4.37 ± 0.03[a]	4.12 ± 0.06[b]
11	Arginylthreonine	C10H21N5O4	1.219366598	0.946438746	0.0314	4.98 ± 0.03[b]	5.26 ± 0.06[a]
12	3'-Amino-3'-deoxythimidine	C10H15N3O4	2.141710248	1.17818258	0.012	5.62 ± 0.01[a]	4.77 ± 0.13[b]
13	Deoxyinosine	C10H12N4O4	1.051419849	0.963062578	0.01849	5.37 ± 0.01[b]	5.57 ± 0.04[a]
14	Pro Phe Gly	C16H21N3O4	1.296538455	0.94131938	0.01934	5.03 ± 0.01[b]	5.35 ± 0.06[a]
15	2-O-(6-Phospho-alpha-mannosyl)-*D*-glycerate	C9H17O12P	2.585010797	0.830678385	0.007185	6.04 ± 0.07[b]	7.28 ± 0.12[a]
16	CHEBI:69439	C10H16N2O2	1.000568773	1.040916881	0.04043	4.85 ± 0.04[a]	4.66 ± 0.03[b]
17	12'-Apo-b-carotene-3,12'-diol	C25H36O2	1.98899812	0.865766916	0.01605	4.74 ± 0.09[b]	5.48 ± 0.09[a]
18	Leucylproline	C11H20N2O3	1.157301011	1.05078125	0.005794	5.11 ± 0.02[a]	4.86 ± 0.02[b]
19	Hydroxyprolyl-Tyrosine	C14H18N2O5	1.046172764	0.959304623	0.02795	4.85 ± 0.05[b]	5.06 ± 0.01[a]
20	Bufotenin	C12H16N2O	1.005608558	0.962620579	0.003934	4.78 ± 0.01[b]	4.97 ± 0.02[a]
21	2-Propenyl cyclohexanebutanoate	C13H22O2	1.005294987	0.967158412	0.006335	5.50 ± 0.02[b]	5.69 ± 0.01[a]
22	*D*-Pipecolic acid	C6H11NO2	1.350250183	1.05626556	0.01547	6.36 ± 0.03[a]	6.02 ± 0.05[b]
23	LysoPE(0:0/22:5(7Z,10Z,13Z,16Z,19Z))	C27H46NO7P	1.213850046	1.057841141	0.0485	5.19 ± 0.08[a]	4.90 ± 0.02[b]
24	Choline Phosphate	C5H14NO4P	1.12702193	1.050872399	0.03901	4.99 ± 0.01[a]	4.75 ± 0.06[b]
25	LysoPE(22:4(7Z,10Z,13Z,16Z)/0:0)	C27H48NO7P	1.843770463	1.171063367	0.009781	4.30 ± 0.08[a]	3.67 ± 0.04[b]
26	LysoPC(22:4(7Z,10Z,13Z,16Z)/0:0)	C30H54NO7P	1.973672619	1.195911866	0.03222	4.50 ± 0.19[a]	3.76 ± 0.01[b]
27	(3beta,5alpha,6beta,22E,24R)-23-Methylergosta-7,22-diene-3,5,6-triol	C29H48O3	1.034968133	0.970133414	0.002799	6.39 ± 0.01[b]	6.59 ± 0.01[a]
28	Propenoylcarnitine	C10H17NO4	1.202303778	0.964928534	0.000215	7.29 ± 0.01[b]	7.55 ± 0.01[a]
29	PC(O-16:0/0:0)	C24H52NO6P	1.016533196	0.972016819	0.02049	6.70 ± 0.02[b]	6.89 ± 0.03[a]
30	All-trans-Heptaprenyl diphosphate	C35H60O7P2	3.954192267	0.342129417	0.0001855	1.49 ± 0.01[b]	4.35 ± 0.05[a]
31	LysoPC(0:0/18:1(9Z))	C26H52NO7P	1.536982116	1.069140501	0.006619	6.70 ± 0.02[a]	6.30 ± 0.04[b]
32	PE(18:1(9Z)/0:0)	C23H46NO7P	1.154155821	1.049603175	0.02518	5.28 ± 0.02[a]	5.03 ± 0.05[b]
33	LysoPC(0:0/18:2(9Z,12Z))	C26H50NO7P	1.429042681	1.05612778	0.005707	7.07 ± 0.04[a]	6.69 ± 0.01[b]
34	Prolylphenylalanine	C14H18N2O3	1.310092692	1.075401443	0.03078	4.62 ± 0.01[a]	4.29 ± 0.08[b]
35	Prolyl-Valine	C10H18N2O3	1.666231473	0.854166667	0.01883	3.03 ± 0.04[b]	3.55 ± 0.09[a]
36	S-Prenyl-L-cysteine	C8H15NO2S	1.914965883	0.833373994	0.0156	3.41 ± 0.12[b]	4.09 ± 0.01[a]
37	AMRINONE	C10H9N3O	2.170038743	0.58708134	0.0002522	1.22 ± 0.01[b]	2.09 ± 0.01[a]

(*continued on next page*)

Table 3 (*continued*)

No.	Metabolite	Formula	VIP_PLS-DA	FC (BS1/BS2)	P_value	BS1	BS2
38	PE(20:5(5Z,8Z,11Z,14Z,17Z)/18:4(6Z,9Z,12Z,15Z))	C43H68NO8P	2.277099688	0.798957247	0.01413	3.83 ± 0.15[b]	4.79 ± 0.06[a]
39	Prolyl-Methionine	C10H18N2O3S	1.633638602	1.154087065	0.005965	3.68 ± 0.05[a]	3.19 ± 0.01[b]
40	Tetrahydrobiopterin	C9H15N5O3	2.056667875	1.154266745	0.01874	5.91 ± 0.15[a]	5.12 ± 0.02[b]
41	*P*-Aminobenzaldehyde	C7H7NO	1.383396452	1.111144669	0.04689	3.67 ± 0.08[a]	3.31 ± 0.08[b]
42	Homolanthionine	C8H16N2O6S	2.091177653	0.832648871	0.01608	4.05 ± 0.09[b]	4.86 ± 0.11[a]
43	PD-160725 2-hydroxyethanesulfonate	C15H18N4O4	2.400003889	1.280848834	0.01486	4.88 ± 0.18[a]	3.81 ± 0.05[b]
44	5-Hydroxyvalproic acid	C8H16O3	1.825546421	1.151248514	0.04099	4.84 ± 0.18[a]	4.20 ± 0.04[b]
45	Arginylproline	C11H21N5O3	1.367992318	1.07651715	0.01304	4.89 ± 0.04[a]	4.54 ± 0.03[b]
46	Arg Leu	C12H25N5O3	1.153003416	0.948992184	0.0184	4.61 ± 0.04[b]	4.86 ± 0.02[a]
47	Alpha-Campholonic acid	C10H16O3	1.312052764	0.927526292	0.006552	4.05 ± 0.01[b]	4.37 ± 0.03[a]
48	Lys Leu	C12H25N3O3	1.622840214	0.908265213	0.04393	4.99 ± 0.14[b]	5.50 ± 0.06[a]
49	*S*-(1,2-Dicarboxyethyl)glutathione	C14H21N3O10S	1.944781992	0.86951714	0.02007	4.71 ± 0.06[b]	5.42 ± 0.12[a]
50	Glutaminyl-Gamma-glutamate	C10H18N4O5	1.862929156	0.863010753	0.001395	4.01 ± 0.01[b]	4.65 ± 0.03[a]
51	Guanosine 2′-monophosphate	C10H14N5O8P	3.711349376	0.605160281	2.62E-05	3.86 ± 0.01[b]	6.39 ± 0.01[a]
52	L-Serine	C3H7NO3	1.396430066	1.082022472	0.02142	4.81 ± 0.03[a]	4.44 ± 0.07[b]
53	*L*-Alanine	C3H7NO2	1.083539031	1.036273702	0.02193	6.28 ± 0.02[a]	6.06 ± 0.04[b]
54	3-(1-Pyrazolyl)-Alanine	C6H9N3O2	1.182113049	1.041456494	0.02739	6.60 ± 0.03[a]	6.34 ± 0.05[b]
55	P-TOLUENESULFONYL FLUORIDE	C7H7FO2S	2.006743837	0.855312735	0.03954	4.53 ± 0.01[b]	5.30 ± 0.22[a]
56	1-Methylhistamine	C6H11N3	1.206771926	1.062145611	0.02608	4.68 ± 0.05[a]	4.40 ± 0.04[b]
57	Deoxyhypusine	C10H23N3O2	1.391372831	0.92782282	0.02946	4.69 ± 0.07[b]	5.05 ± 0.05[a]
58	(3*S*)-3,7-Diaminoheptanoic Acid	C7H16N2O2	1.529555837	1.09449811	0.04646	5.21 ± 0.07[a]	4.76 ± 0.12[b]
59	Cadaverine	C5H14N2	2.529538805	1.359101517	0.04958	4.65 ± 0.12[a]	3.42 ± 0.38[b]
60	LysoPC(18:3(6Z,9Z,12Z)/0:0)	C26H48NO7P	1.597157793	1.084696997	0.006423	6.03 ± 0.01[a]	5.56 ± 0.05[b]
61	PC(16:0/0:0)	C24H50NO7P	1.040864018	1.029461756	0.04874	7.26 ± 0.05[a]	7.05 ± 0.03[b]
62	Lactose	C12H22O11	3.706182025	0.622037064	0.04351	4.32 ± 0.79[b]	6.96 ± 0.14[a]

* BS1 and BS2 represent the nonflavored and flavored treatments. The different letters in the same row indicated significant differences ($P < 0.05$).

These findings align with those reported by Tamura et al. (2022) in aged beef, with the observed increase attributed to glycogenolysis in muscle (Komatsu et al., 2020). The observed changes in metabolites may function as potential biomarkers for assessing frozen storage and the aging process (Yu et al., 2021). In the present study, the concentration of organic nitrogen compounds increased with frozen storage, consistent with findings by Tamura et al. (2022), who reported that polyamine levels rise with prolonged aging under refrigeration. This phenomenon is attributed to changes in amines resulting from the decarboxylation of FAAs during postmortem aging (Ngapo & Vachon, 2017).

Figs. 4A, B, and C display the relative content of the metabolites, which mainly included organic acids and derivatives, organic oxygen compounds, lipids, lipid-like molecules, phenylpropanoids, and polyketides at 0 and 3 months. The last major group was replaced by organic nitrogen compounds at 6 months. Primarily the main differential metabolites that were detected only at 0 months of frozen storage were 57 metabolites belonging to different groups, including amino acids, peptides, and analogs (Val-Ile, Met-His, Ser-Val, Tyr-Ser, Asn-Val, *L*-alany-l-valine, alanylmethionine, Liu-Pro-Ala, Val-Asp-Tyr, Val-Val, phenylalanylglycine, Ser-Val-Leu, Phe-Leu, Leu-Pro-Ile, Met-Trp, Met-Phe, Tyr-Phe, Thr-Trp, Phe-Val, Trp-Gln, Val-Phe, Ala-Ile, Tyr-Ala, Ile-Thr, His–Liu–Ala, pyrroline hydroxycarboxylic acid, trandolapril-d5 diketopiperazine, biocytin, 2,3,4,5-tetrahydro-2-pyridinecarboxylic acid, *L*-2,4-diaminobutyric acid, hypusine, and Tyr-Gln); glycerophosphoethanolamines (PE(20:3(8Z,11Z,14Z)/18:4(6Z,9Z,12Z,15Z))); glycerophosphoserines (PS(14:1(9Z)/22:0); PS(14:1(9Z)/22:0)); carbohydrates; carbohydrate conjugates (6-hydroxymelatonin glucuronide and trehalose); purine ribonucleotides (IMP); dicarboxylic acids and derivatives (thiodiacetic acid); steroidal glycosides (tuberoside); terpene lactones (blumealactone *B*); pyrimidine nucleosides (5-fluorouridine); fatty alcohols (oleyl alcohol); monoterpenoids (2-hydroxy-*p*-mentha-1,8-dien-6-one); carbonyl compounds (kynuramine); triterpenoids (notoginsenoside R9); hydroxycinnamic acids and derivatives (*cis*-caffeoyl tartaric acid); guanidines (*p*-hydroxyphenylethylbiguanide); 4-alkoxyphenols (*p*-hydroxymexiletine); steroidal glycosides (tomatine); quinone and hydroquinone lipids (13′-carboxy-gamma-tocopherol); diradylglycerols (3-(2-heptenyloxy)-2-hydroxypropyl undecanoate); naphthofurans (25-*O*-desacetyl rifabutin); cucurbitacins (cucurbitacin

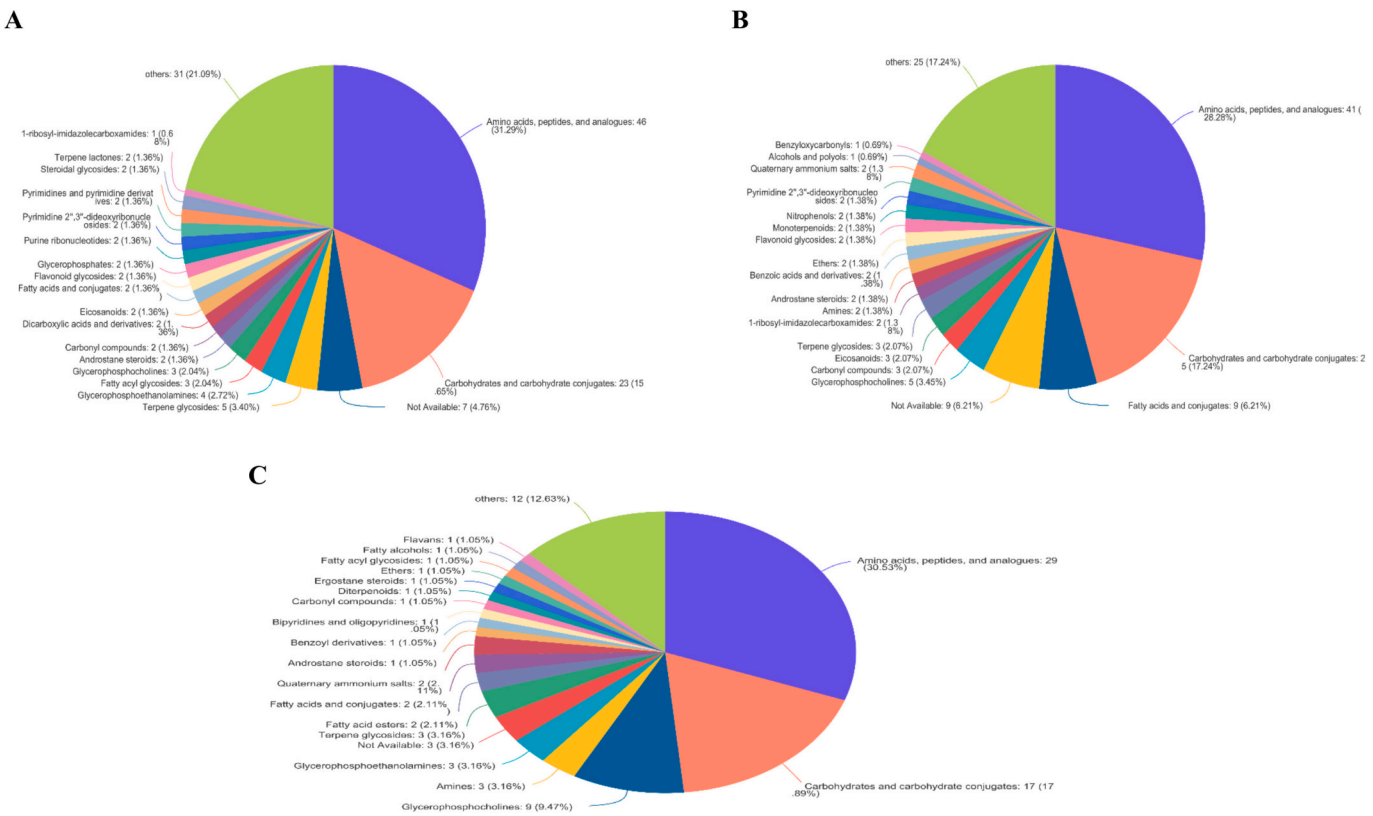

Fig. 4. HMDB metabolites classification of the effectiveness of flavoring substances and freezing processes: A, B, and C, the subclass level of BS1 vs. BS2 at 0, 3, and 6 months of frozen storage periods, respectively.

C); flavonoid glycosides (cyanidin-3,5-diglucoside); phenylpropanoic acids (methyldopa); and gamma butyrolactones (*S*-adenosylhomocysteine) (Table 1). At 3 months of frozen storage, the 43 main differential metabolites detected belonged to different groups, such as fatty acids and conjugates (3-isopropenylpentanedioic acid); purines and purine derivatives (1-methylhypoxanthine); amino acids; peptides; analogs (kainic acid, alanyl-dl-phenylalanine, cyclo(proline-leucine); Tyr-Leu, Gln-Ala-Met, and Tyr-Asn; pyrimidine 2′-deoxyribonucleosides (2′-fluorothymidine); glycerophosphocholines (PC(P-16:0/2:0) and PC(16:1(9Z)/16:0)); fatty acids and conjugates (docosatrienoic acid); and carbonyl compounds (kynuramine and benzoquinone acetic acid) (Table 2). After 6 months of frozen storage, 30 unique metabolites were recognized, including glycerophosphoethanolamines (LysoPE(0:0/22:5(7Z,10Z,13Z,16Z,19Z)), LysoPE(22:4(7Z,10Z,13Z,16Z)/0:0), and PE(18:1(9Z)/0:0)); glycerophosphocholines (LysoPC(18:3(6Z,9Z,12Z)/0:0), PC(O-16:0/0:0), (LysoPC(0:0/18:2(9Z,12Z)), and PC(16:0/0:0)); amines (1-methylhistamine and cadaverine); fatty acid esters (2-propenylcyclohexanebutanoate and propenoylcarnitine); amino acids; peptides; and analogs (1-methylhistidine, arginylthreonine, hydroxyprolyl-tyrosine, polyphenylalanine, prolyl-valine, *S*-prenyl-*L*-cysteine, prolyl-methionine, homolanthionine, arginylproline, and glutaminyl-gamma-glutamate); monoterpenoids (*α*-campholonic acid); benzoyl derivatives (*P*-aminobenzaldehyde); tryptamines and derivatives (bufotenine); and bipyridines and oligopyridines (amrinone) (Table 3). At 0 months, most of the unique differential metabolites belonged to amino acids, peptides, and analogs. At 6 months, many phospholipids were characterized as differential metabolites in the comparison between BSA and BS2 samples, indicating that lipid oxidation occurred slightly during frozen storage, and these substances acted as precursors for flavor formation and enhanced the sensory quality of cooked products. Changes in phospholipids and their correlations with flavor formation can be further evaluated by increasing the frozen storage to up to 12 months. Fig. S2 illustrates the effects of different durations of frozen storage on changes in the metabolite content of the BS1 and BS2 samples. The content of organic oxygen compounds, lipids, and lipid-like molecules increased with frozen storage time in the BS1 and BS2 samples, whereas phenylpropanoids, polyketides, benzoids, and organoheterocyclic compounds decreased with increasing frozen storage time. Carbohydrates, carbohydrate conjugates, organic oxygen compounds, amino acids, peptides, and analogs decreased only in the BS2 sample with increasing frozen storage, indicating that they were consumed as precursors for the chemical interactions among metabolites or were oxidized and degraded during frozen storage.

Meat enzymes can synthesize various amino acids, peptides, and analogs. Enzyme reactions in living organisms occur in the “water phase or at the lipid–water interface” because animal enzymes are water-soluble. Enzyme activity is influenced by a number of factors, including the permeability of the cell membrane, the concentration of water present, and the degree of aggregation polymorphism (Li et al., 2020). In this study, the amount of amino acids and peptides did not show any large variation during frozen storage because of its effect on the enzyme activity. Oxidation occurs continuously in beef, and salt may expedite this process (Mariutti and Bragagnolo, 2017; Al-Dalali et al., 2022a). Oxidation, the loss of electrons, hydrogen detachment, or unpaired electron flow, can happen in all muscle ingredients. The formation of rancid aromas or flavors in previously cooked meats indicates lipid peroxidation. Oxidation of meat colors causes brown discoloration instead of brilliant red. Oxidation of meat proteins reduces their meat-binding, gel-forming, solubility, emulsification, viscosity, and nutritional value. Liu, Liu, et al. (2022) found that protein oxidation causes changes in myofibrillar protein hydrophobic and hydrophilic domains, cross-linking, structural domains, and net protein charge, affecting muscle fiber structure, shear force, spatial arrangement, and water-holding capacity. Food processing may be defined as the physical and chemical alteration of raw food through denaturation, marination, acid reaction, and dehydration. The major processes affecting the

concentrations of metabolites in meat are enzymatic hydrolysis and oxidation (Li et al., 2022). Since oxidation has negative consequences, the majority of research in the meat industry focuses on slowing down oxidative reactions. Oxidation is influenced by endogenous catalysts, antioxidants, and enzymes (Aalhus & Dugan, 2014). Moreover, oxidation rates may be influenced by different actions within the production chain, including the integration of antioxidants into livestock feed, temperature regulation, packaging systems, light exposure, or the direct incorporation of antioxidants, dipeptides, metal chelators, and other substances during processing (Aalhus & Dugan, 2014). In this study, the application of frozen storage is one of the preventive methods that can be used to slow the oxidation processes and enhance meat shelf life.

Microbial growth and oxidation in meat products are linked to consumer rejection. Behbahani et al. (2021) found that all sensory characteristics of beef declined gradually over 7 days of chilled storage, regardless of whether they were coated with active CEO-loaded LPSM edible film. The antioxidant and antimicrobial properties of the oil, along with the oxygen and water barrier characteristics of the edible film, prevent oxidation and growth of bacteria, thereby preventing quality loss in meat (Behbahani et al., 2021). However, the potential involvement of oxidation and microbial activity necessitates further research during frozen storage. In addition, studies extending the frozen storage time to up to 1 year and analyzing targeted metabolites, such as lipids and lipid-like molecules, phospholipids, peptides, and amino acids, and the correlation of these metabolites on flavor formation are needed. The incorporation of spices into raw beef prior to frozen storage for the purpose of inhibiting microbial growth and oxidation requires further investigation.

Fig. S3 presents a heatmap that illustrates the metabolite profiles of BS1 and BS2 (VIP $>$ 1). The VIP analysis diagram shown in Fig. S3 shows that the flavoring substances greatly affected the metabolite profiles of BS1 and BS2 samples during frozen storage. Fig. S3A shows 120 differential metabolites with VIP of >1, which were characterized as markers in the BS1 and BS2 samples; 93 metabolites showed the highest abundances in the BS2 sample versus 27 metabolites in the BS1. The flavoring substances (i.e., sugar and salt) markedly contributed to the metabolites. With continuing freezing for up to 3 months, 55 out of 106 differential metabolites were presented in high abundances in the BS2 sample compared with 51 in the BS1 sample (Fig. S3B). After 6 months of frozen storage, the abundances of 31 metabolites in BS2 were higher than those of the other metabolites. In the BS1 sample, 31 metabolites were higher than those of the other metabolites (Fig. S3C). The flavoring substances greatly affected the metabolite profiles of beef. This effect can be attributed to their ability to lower the water content, prevent microbial development, activate or inhibit the activity of biological enzymes, and promote protein and lipid oxidation, leading to a clear change in the metabolite profile of beef. For example, flavoring substances greatly affected the content of lipid and lipid-like molecules because of lipid oxidation and added salt. These findings were consistent with our previous findings (Al-Dalali et al., 2022a, 2022b). A similar behavior was discovered by Liu et al. (2018) in salt-fermented Antarctic krill; the phospholipase activity of the krill increased after the addition of salt. Bourtsala and Galanopoulou (2019) suggested that the observed phenomenon was due to the increased water–lipid interface and lipase relative level and the decrease in free water content in the cured beef. A previous study reported that sodium chloride (NaCl) and sodium lactate (NaL), alone (30 g/kg) or in combination (20 + 20 g/kg), have been evaluated on raw ground beef's microbiological during chilled storage at 2 °C. The incorporation of NaL or mixed with NaCl greatly slowed the growth of psychrotrophic counts, aerobic plate counts, Enterobacteriaceae, and lactic acid bacteria, and expanded the product's shelf life to 15 and 21 days, respectively, compared to 8 days for control. NaL did not influence TBA-measured lipid oxidation. The oxidative alterations generated by NaCl were greatly decreased by NaL (0.384 vs 0.463). Thus, NaL alone or in conjunction with NaCl may prevent microbiological growth and increase ground beef shelf life under refrigerated storage (Sallam & Samejima, 2004).

The concentrations of many differential metabolites were greater in the BS2 sample than in the BS1 sample at all frozen storage times. The concentrations of lactose in the BS1 and BS2 samples were respectively 3.68 and 7.03 at 0 months, 3.74 and 7.06 at 3 months, and 4.32 and 6.96 at 6 months. Similarly, the concentrations of artemidinol in BS1 and BS2 were respectively 5.89 and 6.39 at 0 months and 3.94 and 6.39 at 3 months. Lastly, the concentrations of trehalose in BS1 and BS2 were respectively 3.8 and 8.11 at 0 months and 4.30 and 8.12 at 3 months. The multivariate statistical analysis indicated that flavoring materials mainly affect the metabolites of raw beef. In addition, flavoring substances showed a greater effect on the content of nine different metabolite groups, including carbohydrates, carbohydrate conjugates, organic oxygen compounds, lipids, lipid-like compounds, organic nitrogen compounds, phenylpropanoids, polyketide, and benzoids (Fig. S2), except nucleosides, nucleotides, and analogs, and amino acids, peptides, and analogs. These results showed that the flavoring of beef with sugar and salt through marination can be used to enhance the flavor, taste, and metabolites of meat. However, further studies are required to investigate the effects of different flavoring substances during frozen storage on the nonvolatile metabolites and volatile flavor components of raw and roasted beef.

The role of differential metabolites in the meat quality

Initially, we conducted a study of all differential metabolites and compiled a list of substances that recognized sensory qualities and/or applications in pharmaceuticals or food as flavor modifiers. Nonvolatile metabolites are significant flavor chemicals and precursors, with their influence on the flavor profile relying upon cooking temperatures. In cooked beef, the primary flavor precursors include peptides, FAAs, nucleotides, sugars, and thiamine (Kaczmarska et al., 2021). L-Carnitine is regarded as a bioactive constituent of meat, contributing to muscular energy metabolism. Choline is a vital vitamin that plays a role in the formation of membrane lipids (Zeisel et al., 1991). Hypoxanthine is produced from purine breakdown and improves the taste of meat (Ichimura et al., 2017). Epsilon-carboxymethyl lysine serves as a prominent advanced glycation end product (AGE) antigen in tissue proteins and may be utilized as a marker for the oxidative degradation of glycated proteins (Reddy et al., 1995). *cis*-Acetylacrylate is an unsaturated acid metabolite that can be produced via carbohydrate metabolism and microbial metabolism in various environments (Liu, Liu, et al., 2022). 2-O-Alpha-*D*-mannopyranosyl-*D*-mannopyranose consists of two mannose units linked by a glycosidic bond exhibiting antigenic properties (Silvia et al., 2007). Melezitose is a trisaccharide that functions to reduce osmotic stress. Phosphoribosyl formamidocarboxamide serves as an intermediate in purine metabolism and is classified as an organic compound. It is a byproduct of ligase activity and is produced by *Escherichia coli* (strain K12). Caftaric acid (*cis*-caffeoyl tartaric acid) is a phenolic compound found in white wine and is recognized for its potential antioxidant properties (Koriem, 2020). Tomatine is a glycoalkaloid utilized for its antifungal properties. Glutamic acid, glutamine, and aspartic acid enhance the savory and umami taste profiles of meat. Glutathione and cysteine serve as significant precursors for the Maillard reaction products that contribute to meat flavor. Some peptides produced enhance the preferred umami taste, particularly glutamyl dipeptides (Kaczmarska et al., 2021). Glycine and serine enhance the experience of umami taste in IMP. Glutamic and aspartic acids are recognized for their contributions to umami taste (Charve et al., 2018). Zhang et al. (2021) reported that phenylalanine and alanine contributed to the irritant taste, lysine (sourness), histidine and creatinine (umami), and pantothenic acid (saltness) in fish meat.

As shown in Tables 1–3, there are many di- and tri-peptides were identified in beef samples. These peptides can improve the quality of beef meat; as documented in the literature, these peptides have bioactive features, including anti-diabetic effects, angiotensin-converting enzyme

inhibition (ACE), and potential reduction of hypertension (Kaczmarska et al., 2021). *L*-2,4-Diaminobutyric acid is predominantly synthesized by glutamic acid decarboxylation and is recognized for its hypotensive and antioxygenic properties in rats. It serves as an inhibitory neurotransmitter and is utilized to alleviate symptoms like drowsiness and autonomic disorders (Kaczmarska et al., 2021).

Conversely, 3′-amino-3′-deoxythymidine (AMT) and 3′-amino-3′-deoxythymidine glucuronide (GAMT) are catabolites identified during three periods of frozen storage, with the exception of GAMT, which was not detected at 6 months of frozen storage. They result from the action of specific enzymatic hydrolysis. Both catabolites exhibit toxicity to human health. Research involving human hematopoietic progenitor cells indicated that AMT was 5- to 7-fold more harmful to human colony-forming units of granulocyte-macrophage and burst-forming units of erythroid compared to 3′-azido-3′-deoxythymidine (Cretton et al., 1991).

PCA and PLS–DA analysis

Unsupervised PCA and supervised PLS–DA were employed to differentiate and screen differential metabolites of the BS1 and BS2 samples. The PCA results indicated that frozen storage considerably affected the metabolites of the BS1 sample, and the identified metabolites were distributed on the left side of PCA. The identified metabolites at 3 and 6 months of frozen storage were distributed close to each other on the right side of PCA (Fig. S4A), indicating that freezing affected the metabolite profile of BS1. The differential metabolites of the BS2 sample were distributed around the center of the PCA axis, showing the effect of frozen storage on the metabolites of BS2 (Fig. S4B). The PCA score plot indicated that PC1 accounted for 52.5 % (BS1) and 38.3 % (BS2) of the total variance, and PC2 for 6.5 % (BS1) and 21.7 % (BS2). PLS–DA were consistent with PCA (Figs. S4C and D) and clearly showed the effect of frozen storage on the metabolites of BS1 and BS2. The distribution of different storage times was clear and far from each other on the four sides of the PLS–DA charts, especially for the BS2 sample. Such findings showed the importance of applying supervised PLS–DA to the study of the effects of frozen storage on the metabolites of samples during different storage periods. The PLS–DA plot indicated that component 1 accounted for 56.6 % (BS1) and 28.6 % (BS2) of the total variance, and component 2 for 10.7 % (BS1) and 22.9 % (BS2) of the total variance. The PLS–DA model has been built and has a strong prediction capacity ($Q^2 > 0.5$; Figs. S4E and F).

KEGG annotation and enrichment analysis of differential metabolites

KEGG annotation and enrichment analysis were performed on the differential metabolites, and their roles in physiological processes and functions were explored (Gu et al., 2021). The 120, 106, and 62 differential metabolites in the comparison between BS1 and BS2 at 0, 3, and 6 months were identified in 33 KEGG pathways (Figs. S5A, B, and C). Six different pathways occurred at 3 months of frozen storage, including the foxO signaling pathway: EIP, cAMP signaling pathway: EIP, pathways of neurodegeneration-multiple diseases: HD, purine metabolism: M, Parkinson's disease: HD, and pentose and glucuronate interconversion: M. In addition, another four pathways occurred at 6 months of frozen storage, including glutathione metabolism: M, aminoacyl–tRNA biosynthesis: GIP, mineral absorption: OS, pantothenate and CoA biosynthesis: M, and biosynthesis of cofactors: M (Fig. S5). The level of enrichment increases with the ratio. At 0 months, 10 signal pathways exhibited an enrichment degree above 0.1. At 3 months, eight signal pathways showed an enrichment value surpassing 0.1. Furthermore, after 6 months of frozen storage, seven signal pathways exhibited an enrichment degree surpassing 0.1 (Fig. S5). The 6, 7, and 9 signal pathways showed high significance at 0.001 in 0, 3, and 6 months of frozen storage (Fig. S5). The results of this study suggested large variations in the physiological metabolism of the muscles throughout different periods of frozen storage. Gu et al. (2021) highlighted the importance of the pathways "insulin resistance (ko04931) and thermogenesis (ko04714)" in relation to the differential abundance of lipids among cattle–yak, yak, and cattle. Liu, Sun, et al. (2022) identified the specific types of metabolites included in beef EXUs that differed from one another. These compounds primarily included organic acids and their derivatives; organoheterocyclic compounds; lipids and lipid-like molecules; benzenoids; phenylpropanoids and polyketides, nucleosides; nucleotides; and their analogs. The primary pathways implicated (top 30) encompassed disease (H, carbon metabolism), environmental information processing (E, ABC transporters and neuroactive ligand–receptor interactions), cellular processes (C, iron death), metabolism (cofactor biosynthesis, purine metabolism, phenylalanine metabolism, M, amino acid biosynthesis), and organismal systems (O, absorption and digestion of protein). Wen et al. (2020) reported that nucleosides and nucleotides play crucial roles in several physiological functions, actively participating in the metabolism of molecules through diverse biochemical reactions. However, only L-glutamine and ADP levels increase during nucleotide metabolism. ATP-related precursors, such as myosin 5′-monophosphate, hypoxanthine, and xanthine, showed a decrease, indicating a down-regulation. This result suggests a connection between energy metabolism and nucleotide synthesis.

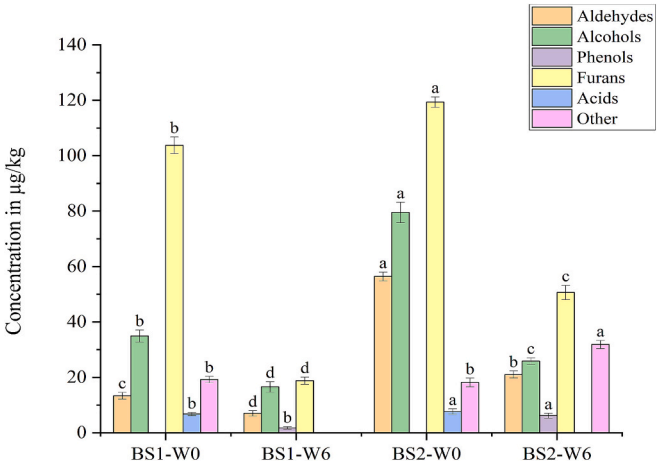

Fig. 5. Changes in the concentrations of different chemical flavor groups (μg/kg) in BS1 and BS2 samples at 0 and 6 months of frozen storage. The different letters upon the same chemical group among the treatments indicated significant differences ($p < 0.05$).

Identification of flavor compounds

The volatile flavor profiles of flavored and nonflavored raw beef samples were qualified through the HS–SPME–GC–MS. A comprehensive analysis revealed 27 volatile compounds in the BS1 and BS2 samples: 16 verified by their authentic compounds and 12 volatiles identified by matching their MS and RI values in two columns with those reported in the NIST library and previous research. The flavor compounds that were identified belonged to a range of chemical families involving aldehydes (8 compounds), alcohols (9), furans (4), phenols (3), ethers (2), and other compounds (1). In addition, 15 volatiles were identified in the BS1 sample and 23 volatiles in the BS2 samples, indicating that the flavoring process enhances the flavor profile of raw beef. Benzeneacetaldehyde, octanal, hexanal, pentadecanal, tetradecanal, hexanol, *trans*-2-octenol, and hexanoic acid were identified only in the BS2 sample. The concentrations of most identified components in the BS1 and BS2 samples decreased after 6 months of frozen storage, except those of *trans*-2-octenal, 1-octen-3-ol, nonanal, anethole, estragole, and 2,6,11-trimethyl-dodecane, which increased in the BS2 sample after freezing for 6 months. Fig. 5 illustrates that the total concentrations of alcohols, aldehydes, furans, and acids were higher in the BS2 sample

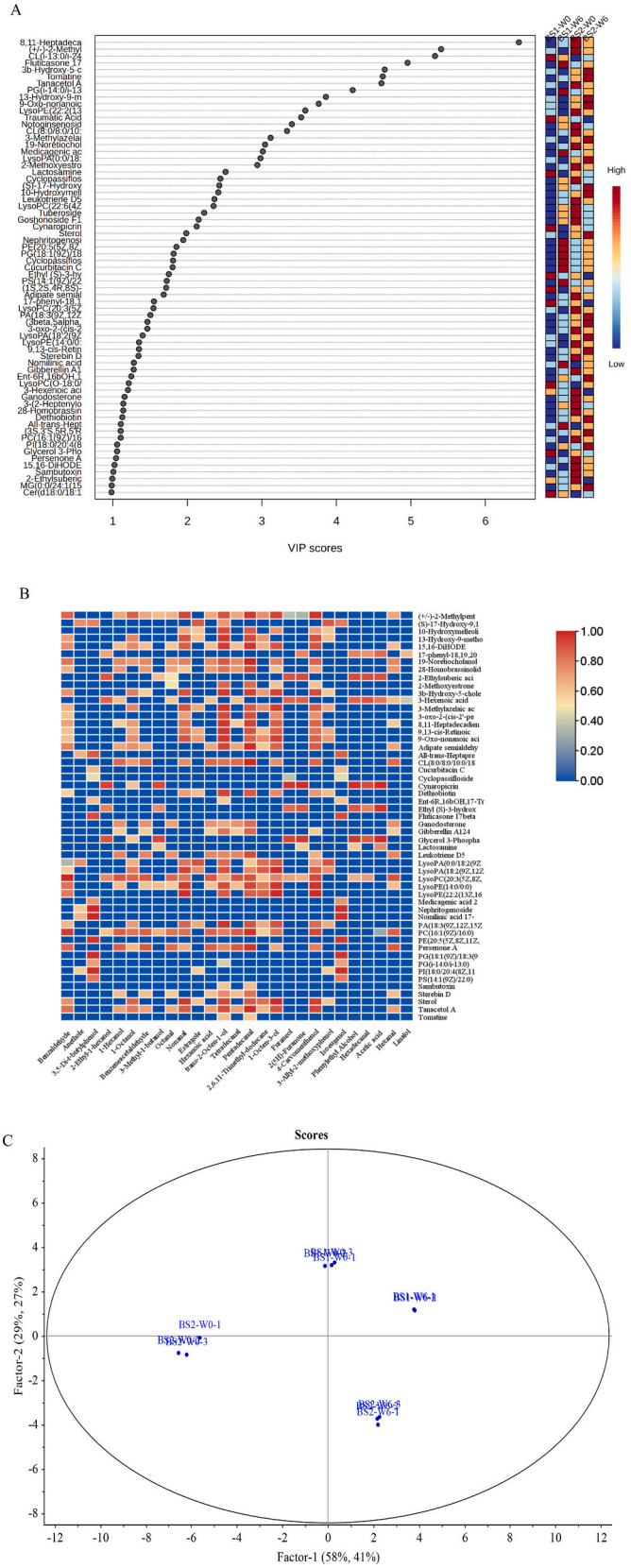

Fig. 6. Correlation analyses: (A) VIP values of 62 markers of lipids and lipid-like molecules that have values higher than 1; (B) correlation of Pearson coefficient between 62 markers of lipids and lipid-like molecules and volatile flavors; (C) PLSR score plot between volatile flavors compounds and lipids and lipid-like molecules; and (D) PLSR correlation loading plot between lipids and lipid-like molecules and volatile flavors.

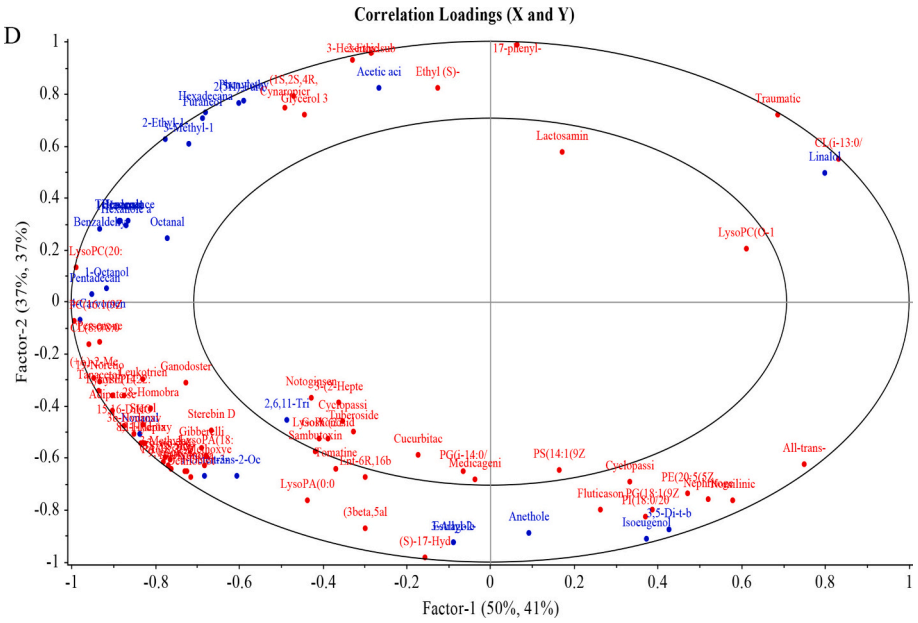

Fig. 6. (*continued*).

than in the BS1 sample. The majority of the screened freeze indicators were aldehydes and alcohols. These components originated from lipid and phospholipid oxidation and fatty acid degradation (Al-Dalali et al., 2022a, 2022b). Their content decreased during frozen storage (Fig. 5). In addition, the following compounds were generated during frozen storage: linalool, anethole, estragole, isoeugenol, and 3,5-di-t-butylphenol. Qi et al. (2021) found that the prolonged storage of raw beef led to temporary increases and decreases in volatile compounds, and ketone and aldehyde levels stabilized. The levels of hydrocarbons, alcohols, esters, and furans fluctuated, and the flavoring process contributed to the content and number of qualified components. The acceleration of lipid oxidation and the creation of chemicals can be linked to the marinade content, such as salt.

Relationship between the differential metabolites and flavor formation

The role of metabolites in flavor formation, small peptides, amino acids, nucleotides, organic acids, and carbohydrates exhibited interactions characterized by either suppressive or synergistic effects. Consequently, the alignment of diverse metabolite components played a significant role in determining the overall flavor and taste profile of dry-cured beef (Fu et al., 2022). The primary sources of volatiles in meat include lipid oxidative decomposition, thiamine degradation, and the Maillard reaction (Al-Dalali et al., 2022a). Hypotheses on the metabolic pathways and expected precursors of the major volatile components were established on the basis of existing research and utilized in conjunction with MetaCyc platforms. The mechanism underlying volatile development in meat was investigated. Flavored raw beef produces flavor components primarily through fatty and amino acid metabolism. Numerous flavor precursors that contribute to the sensory qualities of meat remain to be determined, as meat comprises possibly hundreds of ingredients that affect its flavor and taste attributes (Zhang et al., 2021). The primary metabolic pathways contributing to meat flavor include the metabolism of glutamate, aspartate, alanine, threonine, serine, glycine, hypotaurine, taurine, and purine (Zhang et al., 2021). Meat products often include hexanal, octanal, nonanal, 1-octanol, 1-heptanol, and1-octen-3-ol that are generated from auto-oxidation or enzyme-oxidation of unsaturated fatty acids in beef, such as linolenic, oleic acids, and linoleic. The oxidation of oleic acid produces hydroperoxides, such as 8-, 9-, 10-, 11-, and 13-ROOH, which are further degraded into aldehydes by hydroperoxide lyase (Al-Dalali et al., 2022a; Wu et al., 2020; Yin et al., 2021). For example, nonanal and octanal may be generated by homolyzing 8- and 9-ROOH, respectively. The primary reaction that produces hexanal from linoleic acid is the alkoxy radical scission of 13-ROOH (Al-Dalali et al., 2022a). 1-Octen-3-ol is generated by linoleic and arachidonic acid metabolism (Wu et al., 2020). *L*-Leucine is the main precursor for 3-methyl-1-butanal production and is decomposed by transaminase into α-ketoisocaproic acid and degraded further into 3-methyl-1-butanal by decarboxylase and then into 3-methyl-1-butanol (Wu et al., 2020). The enzyme aldehyde reductase may partly convert aldehydes to alcohols (Al-Dalali et al., 2022a). Most of the identified compounds formed through lipid degradation during frozen storage and the Maillard reaction was prevented under the freezing condition. Tsujihashi et al. (2022) reported that the Maillard reaction system exhibited consistent color change even at freezing temperatures (−24 °C) for an extended duration. This finding suggested that the system could be utilized for the distribution of frozen food. Further studies are needed to investigate the role of the Maillard reaction in flavor formation in frozen meat after long frozen storage (up to 1 year). 1-Hexanol is generated by reducing hexanal or oxidizing linoleic acid (Merlo et al., 2021). Gąsior et al. (2021) stated that phenols are mostly generated by the lignin pyrolysis or the breakdown activities of microorganisms. They are recognized as the unique flavor attributes of smoked food, playing a role in imparting woody and smoky flavors (Al-Dalali et al., 2022a). Furthermore, Gąsior et al. (2021) have documented that the occurrence of phenolic compounds in meat can be attributed to the consumption of grain and/or grass diets.

Correlation analysis between flavor compounds and lipids and lipid-like molecules

After data normalization, the lipids and lipid-like molecules (502 species) in BS1 and BS2 samples at 0 and 6 months of frozen storage were analyzed by PLS-DA to distinguish the more significant molecules in terms of their VIP. Among these, 62 lipids and lipid-like molecules showed VIP >1, as illustrated in Fig. 6A. Then, the Pearson coefficient correlation between these 62 molecules and 27 identified volatile flavors were conducted. After considering the Pearson values higher than 0.2 and *P* values lower than 0.05, the correlation between 53 molecules and 27 flavors was illustrated by heatmap, as depicted in Fig. 6B. Fig. 6B illustrates the positive correlation between flavor components and their precursor from lipids and lipid-like molecules. It can be assumed that

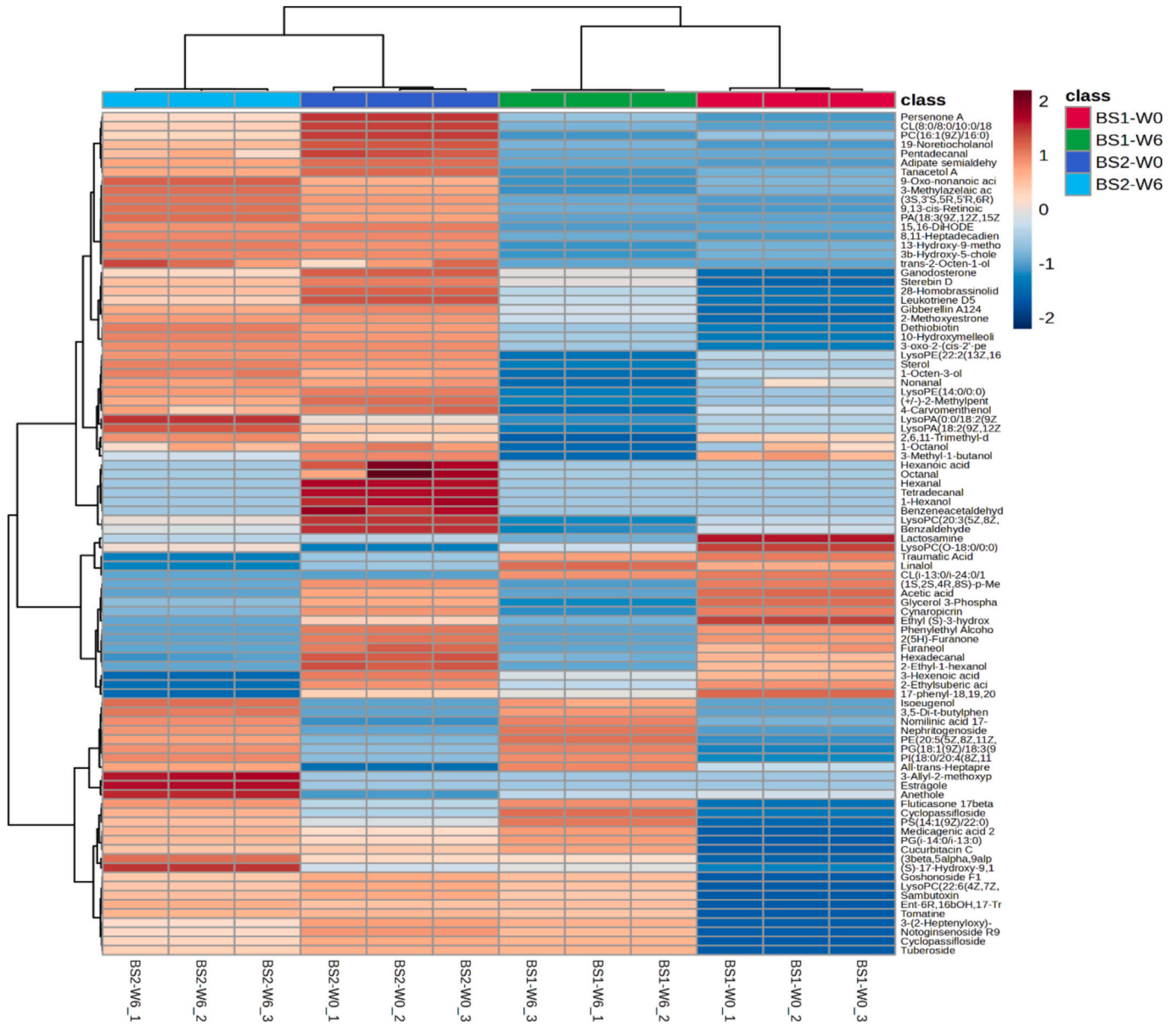

Fig. 7. Heatmap illustrates the distribution of lipids and lipid-like molecules and flavor intensities between BS1 and BS2 samples at 0 and 6 months of frozen storage.

each compound can be generated from different precursors through several pathway mechanisms, especially aldehydes and alcohols. Most of these components were produced through lipid oxidation. It can be seen that about twelve phospholipids showed a positive correlation with the most identified flavor components (Fig. 6B). For example, PC(16:1/(9Z/16:0) showed a positive correlation with hexanal, 4-carvonmethanol, 1-octen-3-ol, pentadecanal, tetradecanal, *trans*-2-octen-1-ol, hexanoic acid, 1-hexanol, and benzaldehyde (Fig. 6B). These findings supported the finding of differential metabolites, in which at 6 months, many phospholipids were recognized as differential metabolites, and these constituents acted as precursors for flavor formation. Further studies are required to study the targeted phospholipids and their correlations with flavor formation.

In addition, the correlations of lipids and lipid-like molecules with flavor changes after frozen storage for 6 months in the flavored and nonflavored beef were visualized with PLSR. The findings of this study provided clear evidence of a correlation between volatile flavor components and lipids and lipid-like molecules (Figs. 6C and D). Factor-1 and factor-2 explained most of the entire variation. BS1 and BS2 at 0 months of freezing were located on the left side of the PLSR diagram, indicating the most volatile characteristics belonged to several chemical groups, including aldehydes (nonanal, hexadecanal), alcohols (phenylethyl alcohol, 2-ethyl-1-hexanol, 1-octen-3-ol, trans-2-octen-1-ol, 4-carvomenthenol), acid (acetic acid), and furan (furaneol) (Fig. 6C). In which, the BS1-W0 located on the upper area of the left side and BS2-W0 located in the lower area of the left side, indicating that the flavoring substances contributed to the enhanced flavor profile of beef. On the right side of the PLSR diagram, BS1-W6 and BS2-W6 were distributed far from each other, and both samples showed the same distribution at 0 months, indicating that the flavor substances contributed to the enriched flavor profile of flavored beef. Fig. 6D also illustrates the positive correlation between identified flavor components and their precursor from lipids and lipid-like molecules. These findings are compatible with the results of flavor analysis by GC–MS. Fig. 7 illustrates the differences in intensities of 62 lipids and lipid-like molecules and flavors between the samples.

Conclusion

A total of 1791 metabolites were identified by UPLC–MS/MS using biochemical databases. The metabolites were classified into 15 groups, including organic acids and derivatives (30.97 %); lipids and lipid-like compounds (33.87 %); organoheterocyclic compounds (13.09 %); organic oxygen compounds (7.49 %); nucleosides, nucleotides, and analogs (4.39 %); benzenoids (4.32 %); phenylpropanoids and polyketides (2.50 %); organic nitrogen compounds (2.09 %); alkaloids and derivatives (0.61 %); hydrocarbons (0.20 %); homogeneous nonmetal compounds (0.13 %); hydrocarbons derivatives (0.07 %); lignans, neolignans and related compounds (0.07 %); organosulfur compounds (0.07 %); and not available (0.13 %). Through PCA and PLS–DA, 120 differential metabolites were found at 0 months of frozen storage, and 94 of these metabolites had higher concentrations in BS2 than in BS1. At 3 months of frozen storage, it was discovered that 55 differential metabolites out of 106 had higher concentrations in BS2 than in BS1. After 6 months of frozen storage, 31 differential metabolites had higher concentrations in BS2 than in BS1. Multivariate statistical analysis and data visualization showed that flavorings considerably affected the metabolites. The organic oxygen compounds, lipids, and lipid-like molecules in the BS1 and BS2 samples increased with frozen storage times, whereas phenylpropanoids and polyketide, benzoids, and organoheterocyclic compounds decreased. Additional research is necessary to examine the effects of various flavoring substances on the nonvolatile metabolites and volatile flavor compounds of raw and roasted beef during frozen storage. Furthermore, the effects of 1 year of frozen storage must be explored, and research should focus on analyzing specific metabolites, such as lipids and lipid-like molecules, phospholipids, peptides, and amino acids. Additionally, it is important to examine the relationship of these metabolites with the formation of flavors.

Ethical approval

This article does not contain any studies with human participants or animals performed by any of the authors.

CRediT authorship contribution statement

Sam Al-Dalali: Writing – review & editing, Writing – original draft, Visualization, Validation, Software, Resources, Methodology, Investigation, Formal analysis, Data curation, Conceptualization. **Zhigui He:** Investigation, Funding acquisition. **Miying Du:** Investigation. **Hui Sun:** Investigation. **Dong Zhao:** Investigation. **Cong Li:** Visualization. **Peijun Li:** Investigation. **Baocai Xu:** Resources, Investigation.

Declaration of competing interest

The authors declare that they have no known competing financial interests or personal relationships that could have appeared to influence the work reported in this paper.

Data availability

Data will be made available on request.

Acknowledgment

This work was financially supported by the Guangxi Zhuang Autonomous Region level financial science and technology plan project Guangxi Key Research and Development Plan (AB19110023) and the Regional Innovation Cooperation Project of Sichuan province (2024YFHZ0207).

Supplementary data

Supplementary data to this article can be found online at https://doi.org/10.1016/j.fochx.2024.101898.

References

Aalhus, J., & Dugan, M. (2014). Encyclopedia of meat sciences || spoilage, factors affecting | oxidative and enzymatic. *Crown Copyright*, 394–400. https://doi.org/10.1016/b978-0-12-384731-7.00091-x

Al-Dalali, S., Li, C., & Xu, B. (2021). Evaluation of the effect of marination in different seasoning recipes on the flavor profile of roasted beef meat via chemical and sensory analysis. *Journal of Food Biochemistry*. , Article e13962. https://doi.org/10.1111/jfbc.13962

Al-Dalali, S., Li, C., & Xu, B. (2022a). Effect of frozen storage on the lipid oxidation, protein oxidation, and flavor profile of marinated raw beef meat. *Food Chemistry, 376*, Article 131881. https://doi.org/10.1016/j.foodchem.2021.131881

Al-Dalali, S., Li, C., & Xu, B. (2022b). Insight into the effect of frozen storage on the changes in volatile aldehydes and alcohols of marinated roasted beef meat: Potential mechanisms of their formation. *Food Chemistry, 385*, Article 132629. https://doi.org/10.1016/j.foodchem.2022.132629

Antonelo, D. S., Gómez, J. F. M., Cônsolo, N. R. B., Beline, M., Colnago, L. A., Schilling, M. W., Zhang, X., Suman, S. P., Gerrard, D. E., Baileiro, J. C. C., & Silva, S. L. (2020). Metabolites and metabolic pathways correlated with beef tenderness. *Meat and Muscle Biology, 4*(1), 1–9. https://doi.org/10.22175/mmb.10854, 19.

Behbahani, B. A., Falah, F., Vasiee, A., & Yazdi, F. T. (2021). Control of microbial growth and lipid oxidation in beef using a Lepidium perfoliatum seed mucilage edible coating incorporated with chicory essential oil. *Food Science & Nutrition, 9*, 2458–2467.

Bourtsala, A., & Galanopoulou, D. (2019). Phospholipases. *Encyclopedia of Food Chemistry*, 277–286. https://doi.org/10.1016/B978-0-08-100596-5.21651-X

Charve, J., Manganiello, S., & Glabasnia, A. (2018). Analysis of umami taste compounds in a fermented corn sauce by means of sensory-guided fractionation. *Journal of Agricultural and Food Chemistry, 66*, 1863–1871.

Cretton, E. M., Xie, M. Y., Bevan, R. J., Goudgaon, N. M., Schinazi, R. F., & Sommadossi, J. P. (1991). Catabolism of 3′-azido-3′-deoxythymidine in hepatocytes and liver microsomes, with evidence of formation of 3′-amino-3′-deoxythymidine, a highly toxic catabolite for human bone marrow cells. *Molecular Pharmacology, 39*(2), 258–266.

Etiévant, P., Guichard, E., Salles, C., & Voilley, A. (2016). *In Flavor*. Woodhead Publishing. https://doi.org/10.1016/B978-0-08-100295-7.00004-9

Felderhoff, C., Lyford, C., Malaga, J., Polkinghorne, R., Brooks, C., Garmyn, A., & Miller, M. (2020). Beef quality preferences: Factors driving consumer satisfaction. *Foods, 9*, 289. https://doi.org/10.3390/foods9030289

Fu, H., Pan, L., Wang, J., Zhao, J., Guo, X., Chen, J., Lu, S., Dong, J., & Wang, Q. (2022). Sensory properties and main differential metabolites influencing the taste quality of dry-cured beef during processing. *Foods, 11*(4), 531. https://doi.org/10.3390/foods11040531

Gąsior, R., Wojtycza, K., Majcher, M. A., Bielinska, H., Odrzywolska, A., Bączkowicz, M., & Migdał, W. (2021). Key aroma compounds in roasted white Kołuda goose. *Journal of Agricultural and Food Chemistry, 69*(21), 5986–5996. https://doi.org/10.1021/acs.jafc.1c01475

Gu, X., Sun, W., Yi, K., Yang, L., Chi, F., Luo, Z., Wang, J., Zhang, J., Wang, W., Yang, T., & Geng, F. (2021). Comparison of muscle lipidomes between cattle-yak, yak, and cattle using UPLC–MS/MS. *Journal of Food Composition and Analysis, 103*, Article 104113. https://doi.org/10.1016/j.jfca.2021.104113

Ichimura, S., Nakamura, Y., Yoshida, Y., & Hattori, A. (2017). Hypoxanthine enhances the cured meat taste. *Animal Science Journal, 88*, 379–385.

Ijaz, M., Zhang, D., Hou, C., Mahmood, M., Hussain, Z., Zheng, X., & Li, X. (2022). Changes in postmortem metabolites profile of atypical and typical DFD beef. *Meat Science, 193*, Article 108922. https://doi.org/10.1016/j.meatsci.2022.108922

Jiang, S., Zhu, Y., Peng, J., Zhang, Y., Zhang, W., & Liu, Y. (2023). Characterization of stewed beef by sensory evaluation and multiple intelligent sensory technologies combined with chemometrics methods. *Food Chemistry, 408*, Article 135193. https://doi.org/10.1016/j.foodchem.2022.135193

Kaczmarska, K., Taylor, M., Piyasiri, U., & Frank, D. (2021). Flavor and metabolite profiles of meat, meat substitutes, and traditional plant-based high-protein food products available in Australia. *Foods, 10*, 801. https://doi.org/10.3390/foods10040801

Komatsu, T., Komatsu, M., & Shoji, N. (2020). Changes in glycogen and monosaccharide during aging of Japanese black cattle beef. *Nihon Chikusan Gakkaiho, 91*, 119–125. https://doi.org/10.2508/chikusan.91.119

Koriem, K. M. M. (2020). Caftaric acid: An overview on its structure, daily consumption, bioavailability and pharmacological effects. *Biointerface Research in Applied Chemistry, 10*(3), 5616–5623. https://doi.org/10.33263/BRIAC103.616623

Lacalle-Bergeron, L., Izquierdo-Sandoval, D., Sancho, J. V., López, F. J., Hern'andez, F., & Portol'es, T. (2021). Chromatography hyphenated to high resolution mass spectrometry in untargeted metabolomics for investigation of food (bio)markers. *TrAC Trends in Analytical Chemistry, 135*. https://doi.org/10.1016/j.trac.2020.116161

Li, C., Al-Dalali, S., Zhou, H., & Xu, B. (2022). Influence of curing on the metabolite profile of water-boiled salted duck. *Food Chemistry, 397*, Article 133752. https://doi.org/10.1016/j.foodchem.2022.133752

Li, C., Li, X., Huang, Q., Zhou, Y., Xu, B., & Wang, Z. (2020). Influence of salt content used for dry-curing on Lipidomic profiles during the processing of water-boiled salted duck. *Journal of Agricultural and Food Chemistry, 68*(13), 4017–4026. https://doi.org/10.1021/acs.jafc.0c01513

Liu, C., Ge, J., Zhou, Y., Thirumurugan, R., Gao, Q., & Dong, S. (2020). Effects of decreasing temperature on phospholipid fatty acid composition of different tissues and hematology in Atlantic salmon (Salmo salar). *Aquaculture, 515*, Article 734587. https://doi.org/10.1016/j.aquaculture.2019.734587

Liu, E., Sun, M., He, C., Mao, K., Li, Q., Zhang, J., Wu, D., Wang, S., Zheng, C., Li, W., Gong, S., Xue, F., & Wu, H. (2022). Rumen microbial metabolic responses of dairy cows to the honeycomb flavonoids supplement under heat-stress conditions. *Frontiers in Veterinary Science, 9*, Article 845911. https://doi.org/10.3389/fvets.2022.845911

Liu, J., Hu, Z., Zheng, A., Ma, Q., & Liu, D. (2022). Identification of exudate metabolites associated with quality in beef during refrigeration. *LWT- Food Science and Technology, 172*, Article 114241. https://doi.org/10.1016/j.lwt.2022.114241

Liu, J., Liu, D., Zheng, A., & Ma, Q. (2022). Haem-mediated protein oxidation affects water-holding capacity of beef during refrigerated storage. *Food Chemistry: X, 14*, Article 100304. https://doi.org/10.1016/j.fochx.2022.100304

Liu, Y., Tian, Y., Cong, P., Chen, Q., Li, H., Fan, Y., & Xue, C. (2018). Lipid degradation during salt-fermented antarctic krill paste processing and their relationship with lipase and phospholipase activities. *European Journal of Lipid Science and Technology, 120*(4), 1700443. https://doi.org/10.1002/ejlt.201700443

Mariutti, L. R., & Bragagnolo, N. (2017). Influence of salt on lipid oxidation in meat and seafood products: A review. *Food Research International, 94*, 90–100. https://doi.org/10.1016/j.foodres.2017.02.003

Merlo, T. C., Lorenzo, J. M., Saldana, E., Patinho, I., Oliveira, A. C., Menegali, B. S., … Contreras-Castillo, C. J. (2021). Relationship between volatile organic compounds, free amino acids, and sensory profile of smoked bacon. *Meat Science, 181*, Article 108596. https://doi.org/10.1016/j.meatsci.2021.108596

Monin, G., Hortós, M., Diaz, I., Rock, E., & Garcia-Regueiro, J. (2003). Lipolysis and lipid oxidation during chilled storage of meat from large white and Pietrain pigs. *Meat Science, 64*, 7–12. https://doi.org/10.1016/S0309-1740(02)00130-4

Ngapo, T. M., & Vachon, L. (2017). Biogenic amine concentrations and evolution in "chilled" Canadian pork for the Japanese market. *Food Chemistry, 233*, 500–506. https://doi.org/10.1016/j.foodchem.2017.04.120

Overholt, M. F., Mancini, S., Galloway, H. O., Preziuso, G., Dilger, A. C., & Boler, D. D. (2016). Effects of salt purity on lipid oxidation, sensory characteristics, and textural properties of fresh, ground pork patties. *LWT- Food Science and Technology, 65*, 890–896. https://doi.org/10.1016/j.lwt.2015.08.067

Parijadi, A. A., Ridwani, S., Dwivany, F. M., Putri, S. P., & Fukusaki, E. (2019). A metabolomics-based approach for the evaluation of off-tree ripening conditions and different postharvest treatments in mangosteen (Garcinia mangostana). *Metabolomics, 15*(5), 73. https://doi. https://doi.org/10.1007/s11306-019-1526-1.

Park, J. Y., Eom, J. U., Parvin, R., Seo, J.-K., Kim, H.-W., & Yang, H.-S. (2022). Changes of volatile and non-volatile metabolites in beef *M. Longissimus Lumborum* under aerobic storage condition. *Journal of Agriculture & Life Science, 56*(2), 85–95. https://doi.org/10.14397/jals.2022.56.2.85

Pezzatti, J., Boccard, J., Codesido, S., Gagnebin, Y., Joshi, A., Picard, D., & Rudaz, S. (2020). Implementation of liquid chromatography-high resolution mass spectrometry methods for untargeted metabolomic analyses of biological samples: A tutorial. *Analytica Chimica Acta, 1105*, 28–44. https://doi.org/10.1016/j.aca.2019.12.062

Putri, S. P., & Fukusaki, E. (2016). *Mass spectrometry-based metabolomics: A practical guide* (p. 3e8). Boca Raton: CRC Press.

Putri, S. P., Ikram, M. M. M., Sato, A., Dahlan, H. A., Rahmawati, D., Ohto, Y., & Fukusaki, E. (2022). Application of gas chromatography-mass spectrometry-based metabolomics in food science and technology. *Journal of Bioscience and Bioengineering, 133*(5), 425–435. https://doi.org/10.1016/j.jbiosc.2022.01.011

Qi, J., Xu, Y., Zhang, W., Xie, X., Xiong, G., & Xu, X. (2021). Short-term frozen storage of raw chicken meat improves its flavor traits upon stewing. *LWT–Food Science and Technology, 142*, Article 111029. https://doi.org/10.1016/j.lwt.2021.111029

Ramalingam, V., Zhen, S., & Hwang, I. (2019). The potential role of secondary metabolites in modulating the flavor and taste of the meat. *Food Research International, 122*, 174–182. https://doi.org/10.1016/j.foodres.2019.04.007

Ramanathan, R., Kiyimba, F., Suman, S. P., & Mafi, G. G. (2023). The potential of metabolomics in meat science: Current applications, trends, and challenges. *Journal of Proteomics, 283-284*. https://doi.org/10.1016/j.jprot.2023.104926

Reddy, S., Bichler, J., Wells-Knecht, K. J., Thorpe, S. R., & Baynes, J. W. (1995). N. Epsilon.-(carboxymethyl)lysine is a dominant advanced glycation end product (age) antigen in tissue proteins. *Biochemistry, 34*, 10872–10878. https://doi.org/10.1021/bi00034a021

Resconi, V. C., Escudero, A., & Campo, M. M. (2013). The development of aromas in ruminant meat. *Molecules, 18*(6), 6748–6781. https://doi.org/10.3390/molecules18066748

Rizo, J., Guillen, D., Farres, A., Diaz-Ruiz, G., Sanchez, S., Wacher, C., & Rodriguez-Sanoja, R. (2020). Omics in traditional vegetable fermented foods and beverages. *Critical Reviews in Food Science and Nutrition, 60*(5), 791–809. https://doi.org/10.1080/10408398.2018.1551189

Sallam, K. I., & Samejima, K. (2004). Microbiological and chemical quality of ground beef treated with sodium lactate and sodium chloride during refrigerated storage. *Lebenson Wiss Technology, 37*(8), 865–871.

Setyabrata, D., Vierck, K., Sheets, T. R., Legako, J. F., Cooper, B. R., Johnson, T. A., & Kim, Y. H. B. (2022). Characterizing the flavor precursors and liberation mechanisms of various dry-aging methods in cull beef loins using metabolomics and microbiome approaches. *Metabolites, 12*, 472, 10.339/metabo12060472.

Silvia, M., Inmaculada, S. M., Pierangelo, M., Laura, B., Jesús, J. B., & Anna, B. (2007). Synthesis and conformational analysis of an α-D-mannopyranosyl-(1–2)-α-D-mannopyranosyl-(1–6)-α-D-mannopyranose mimic. *Carbohydrate Research, 342*(12–13), 1859–1868. https://doi.org/10.1016/j.carres.2007.03.019

Sun, Y., Zhang, Y., & Song, H. (2020). Variation of aroma components during frozen storage of cooked beef balls by SPME and SAFE coupled with GC-O-MS. *Journal of Food Processing and Preservation, 45*(1), Article e15036. https://doi.org/10.1111/jfpp.15036

Tamura, Y., Iwatoh, S., Miyaura, K., Asikin, Y., & Kusano, M. (2022). Metabolomic profiling reveals the relationship between taste-related metabolites and roasted aroma in aged pork. *LWT- Food Science and Technology, 155*, Article 112928. https://doi.org/10.1016/j.lwt.2021.112928

Tsujihashi, M., Tanaka, S., Koyama, K., & Koseki, S. (2022). Application of time–temperature indicator/integrator based on the Maillard reaction to frozen food distribution. *Food and Bioprocess Technology, 15*, 1343–1358. https://doi.org/10.1007/s11947-022-02821-4

Utpott, M., Rodrigues, E., Rios, A. O., Mercali, G. D., & Flores, S. H. (2022). Metabolomics: An analytical technique for food processing evaluation. *Food Chemistry, 366*, Article 130685. https://doi.org/10.1016/j.foodchem.2021.130685

Wen, D., Liu, Y., & Yu, Q. (2020). Metabolomic approach to measuring quality of chilled chicken meat during storage. *Poultry Science, 99*(5), 2543–2554. https://doi.org/10.1016/j.psj.2019.11.070

Wu, S., Yang, J., Dong, H., Liu, Q., Li, X., Zeng, X., & Bai, W. (2020). Key aroma compounds of Chinese dry-cured Spanish mackerel (Scomberomorus niphonius) and their potential metabolic mechanisms. *Food Chemistry, 342*, Article 128381. https://doi.org/10.1016/j. foodchem.2020.128381

Yin, X., Wen, R., Sun, F., Wang, Y., Kong, B., & Chen, Q. (2021). Collaborative analysis on differences in volatile compounds of Harbin red sausages smoked with different types of woodchips based on gas chromatography–mass spectrometry combined with electronic nose. *LWT-food. Science and Technology, 143*, Article 111144. https://doi.org/10.1016/j.lwt.2021.111144

Yu, Q., Cooper, B., Sobreira, T., & Brad Kim, Y. H. (2021). Utilizing pork exudate metabolomics to reveal the impact of aging on meat quality. *Foods, 10*(3). https://doi.org/10.3390/foods10030668

Zeisel, S. H., Da Costa, K.-A., Franklin, P. D., Alexander, E. A., Lamont, J. T., Sheard, N. F., & Beiser, A. (1991). Choline, an essential nutrient for humans. *FASEB Journal, 5*, 2093–2098.

Zhang, T., Chen, C., Xie, K., Wang, J., & Pan, Z. (2021). Current state of metabolomics research in meat quality analysis and authentication. *Foods, 10*, 2388. https://doi.org/10.3390/foods10102388